ABSTRACT

Title:
A CHEMICAL AND ISOTOPIC COMPARISON OF TWO 1ST-ORDER AGRICULTURAL TRIBUTARIES, KENT COUNTY, MARYLAND

Jennifer Teerlink, Master of Science, 2005

Directed By:
Professor Philip Candela, Geology Department

Nitrate derived predominantly from agricultural fertilizers results in algal blooms and wide-spread anoxia in estuarine environments. Roughly half the nitrate delivered to the Chesapeake Bay is derived from groundwater (residence time up to 40 years). Two 1st-order tributaries in eastern Maryland were sampled on five dates. Over the study interval, average nitrate, alkalinity, and $\delta^{13}C$ were 207 µM, 212 µM, and -12.1‰, respectively, in the ditched tributary, and 106 µM, 451 µM, and -9.7‰, respectively, in the unaltered tributary.

Ditching of the western tributary results in discharge of less anthropogenically-altered groundwater. Nitrate, calcium, and magnesium concentrations decrease and ^{13}C abundance of DIC becomes enriched along the reach. The unaltered tributary is stagnant in the headwaters, resulting in consumption of dissolved oxygen and denitrification. Alkalinity correspondingly increases suggesting reduced carbon as the electron source for this microbial process. Alteration of 1st-order tributaries influences the processing and delivery of nutrients.

A CHEMICAL AND ISOTOPIC COMPARISON OF TWO 1ST-ORDER
AGRICULTURAL TRIBUTARIES, KENT COUNTY, MARYLAND

By

Jennifer Teerlink

Thesis submitted to the Faculty of the Graduate School of the
University of Maryland, College Park, in partial fulfillment
of the requirements for the degree of
Master of Science
2005

Advisory Committee:
Professor Philip Candela, Chair
Associate Professor Alan Jay Kaufman
Associate Professor Karen Prestegaard

Dedication

To my Mother, Karen Melby Teerlink

For her unwavering support and enthusiasm

Acknowledgements

There have been many people who have helped me along this path toward completing a Master of Science in Hydrogeology. First and foremost I would like to thank my committee members. Phil Candela maintains the highest standard of quality in scientific investigations. His example and guidance have been invaluable. Jay Kaufman has spent numerous hours thinking through the science behind the isotopic portion of this project. His willingness to work through the methodology of dissolved inorganic carbon isotopic analysis despite the numerous problems was incredible. Karen Prestegaard provided vast background knowledge of hydrogeology, as well as unique and innovative solutions to challenges encountered.

The research conducted wouldn't have been possible without the financial and physical support of many. The Geological Society of America funded two separate student research grants for this work. Jay Kaufman's gas source mass spectrometer was used for all isotopic analysis. Phil Candela's Atomic Absorption Spectrophotometer was used for all cation analysis. Karen Prestegaard's field equipment was used to characterize the study site. My field site was on the property of Angelica Nurseries. Jim Kohl willingness to allow me to work on his land was invaluable.

Numerous professors enhanced my understanding of the scientific process through quality graduate courses including Phil Candela, James Farquhar, Rich Walker, Jennifer Becker, Alba Torrents, Kaye Brubaker, Jay Kaufman, and Karen Prestegaard. Each graduate student at the University of Maryland works largely independently, however the challenge provided in courses and the ever present offer

Table of Contents

List of Tables

List of Figures

Chapter 1: Defining the Problem

1.1 Introduction

The Chesapeake Bay, the largest and most productive estuary in the United States, is of significant economic, recreational, and environmental importance. The productivity of the bay; however, is compromised by the delivery of excess nutrients from watershed tributaries. Nutrients derived from fertilizers, the atmosphere, and the burning of fossil fuels nourish algal blooms that block sunlight to estuary grasses. Once these blooms die, they sink and decay. This process depletes the water of dissolved oxygen and creates widespread anoxia, thereby killing fish and other aquatic organisms. This process is known as eutrophication (Zynjuk, 1995; Moffatt, 1998). Excess nitrate in drinking water also poses a health risk to residents. The anoxia that results from eutrophication has stressed the ecosystem (Bachman et al., 2002). Management practices that strive to reduce nutrient fluxes to the bay should be based on an in-depth understanding of the watershed processes that both deliver and reduce nutrient loads to downstream sites.

Phosphorous and nitrogen, the two primary components of fertilizer, interact differently with soil and water. In oxidized environments, phosphorous adsorbs to soil, while nitrate remains highly soluble (Bachman et al., 2002). Nitrogen, while abundant in the atmosphere, must be fixed as nitrate to be bioavailable. Until the turn of the century, fixed nitrogen was produced dominantly by soil microbes or lightning. The resulting flux of nitrate was largely consumed as it moved through the system. With the introduction of synthesized fertilizers, however, the nitrogen load exceeded

that required for plant growth (Moffat, 1998), resulting in the delivery of excess fixed nitrogen to estuaries and bays.

Groundwater accounts for 60 to 80 percent of total stream flow within the Chesapeake drainage (Shedlock, 1993). Programs designed to decrease nitrogen flux to estuaries and lakes have helped to slow down the application of fertilizers; however, over 50 years of use has resulted in the accumulation of excess nitrogen in shallow groundwater and soils in agricultural regions of the Chesapeake drainage area (Bolhke and Denver, 1995; Bachman et al., 2002). Phillips et al. (1999) have quantified the groundwater nitrate contribution as about half of nitrate flux to the bay; thus nitrate in subsurface reservoirs plays a major role in total flux of nutrients. Notably, groundwater discharging in the Chesapeake drainage is up to 40 years in age (Focazio et al., 1998). Considering the substantial time lag between recharge and discharge, it is likely that nutrient concentrations and chemical compositions of shallow aquifers might vary as a function of microbial interactions.

Nitrate concentrations in the Delmarva aquifers also impose a potential health risk for residents. Groundwater samples taken in the Delmarva Peninsula commonly exceed the Environmental Protection Agency's (EPA) Maximum Contaminant Level (MCL) of 10 mg/L. Groundwater wells used for private consumption put infants under the age of six months at risk for developing *methemoglobinemia* also known as blue baby syndrome (Bachman et al., 2002), which interferes with the delivery of oxygen to the brain and other tissues, sometimes resulting in death.

There is no minimum nitrate concentration for eutrophication; rather the forcing functions are the rate of total delivery of nutrients to a water body relative to

its size. Between 1990 and 1992, the Chesapeake Bay received over 600 million pounds of nitrogen, enough to continue the nourishment of algal blooms and widespread anoxia (Zynjuk, 1995).

Surface water chemistry is driven by the interaction between geologic, biologic, atmospheric, and hydrologic parameters. The incoming groundwater carries with it the chemical signature of its recent geologic history. Depending upon its flow path, the chemical composition of the groundwater may be altered by interactions with sediments, bacteria, plants, animals and atmospheric gases. The flow path of that water and the residence time within any individual reservoir will dictate what interactions occur. Nitrate concentrations are especially affected by this dynamic interaction, but other chemical parameters must also be monitored to fully characterize the system.

Nitrate loading to estuaries and bays poses a great environmental and economic risk. Management has focused on how to reduce nitrate flux by decreasing the use of fertilizer (Phillips and Lindsey, 2003). Present-day management however has only a limited immediate impact as much of the damage to the Delmarva aquifers has already occurred. The high solubility of nitrate and its long residence time in groundwater results in continual delivery of fossil nitrate to the Chesapeake Bay (Focazio et al., 1998) even as current usage declines. Thus understanding conditions under which nitrate is naturally attenuated enables better management of existing subsurface nitrate reservoirs.

1.2 Biogeochemical Processing in Streams

1.2.1 Denitrification

Denitrification is a biologically-mediated process that can reduce nitrate to molecular nitrogen by the half reaction:

$$6H^+ + NO_3^- + 5e^- \leftrightarrow N_2 + 3H_2O \qquad (1)$$
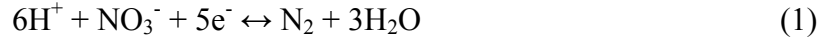
Balanced equations for nitrate reduction with organic carbon, pyrite, or iron oxide, respectively as electron donors are written as

$$2NO_3^- + 2CH_2O \leftrightarrow N_2 + 2HCO_3^- + 2H_2O \qquad (2)$$

$$6NO_3^- + 2FeS_2 + 2H_2O \leftrightarrow 3N_2 + 2FeOOH + 4SO_4^{2-} + 2H^+ \quad (3)$$

$$2NO_3^- + 10FeO + 2H^+ + 4H_2O \leftrightarrow N_2 + 10FeOOH \qquad (4)$$
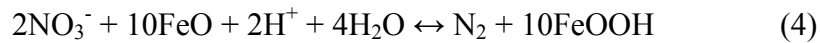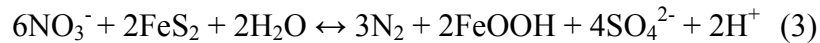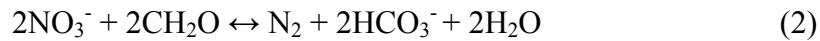
There are several groups of microorganisms that are capable of denitrification, including the genera *Alcaligenes*, *Bacillus*, and *Pseudomonas*. These bacteria are able to respire most efficiently with free oxygen. It is only in the absence of free oxygen, that they can use nitrate as a terminal electron acceptor. Depending upon the bacterial species, there can be several intermediate steps that transform nitrogen between nitrate, nitrite, nitric oxide, nitrous oxide, and molecular nitrogen. However, the nitrate ion is considered the necessary starting point for denitrification and molecular nitrogen the ultimate product (Gerardi, 2002).

Nitrogen isotopes of nitrate have commonly been used to label contributing sources and subsequent biogeochemical transformations such as denitrification (McMahon and Bohlke, 1996; Koba et al., 1997; Chang et al., 2001; Hinkle et al., 2001; Robinson, 2001; Bohlke et al., 2002; Ostrom et al., 2002). Nitrogen has two stable isotopes; ^{14}N and ^{15}N.

$$\delta^{15}N = \frac{\left[^{15}N\right]}{\left[^{14}N + ^{15}N\right]} * 1000 \qquad (5)$$

Biological processes tend to incorporate the lighter isotope leaving the remaining pool enriched. Enrichment in ^{15}N of residual nitrate in groundwater and organic nitrogen in plants is commonly sited as evidence of denitrification (McMahon and Bohlke, 1996; Koba et al., 1997; Hinkle et al, 2001; Bohlke, 2002; Bohlke et al., 2002; Ostrom et al., 2002). Analytical methods used to analyze for nitrate isotopes pose significant challenges. There are two well accepted methods proposed in the literature; 1) precipitation of solid nitrate and 2) the biologically-mediated and quantitative reduction of nitrate back to nitrogen gas. Precipitating enough silver nitrate for analysis using a series of resin exchange columns requires large volumes of water (Silva et al., 2000) and is thus unfeasible in this study. Casciotti et al. (2002) use bacteria to partially reduce nitrate to gaseous nitrous oxide, which can then be analyzed for oxygen and nitrogen isotope abundances. While this method does not require the large volumes of water as in the precipitation method, it does require a lab equipped to handle microbial populations, thus this method isn't feasible for this study.

Many studies have identified and detailed hydrogeologic conditions where denitrification is likely to occur (Burt et al., 2002; Clement et al., 2003; Hinkle et al., 2001; Konohira et al., 2001; Lund et al., 2000; Maitre et al., 2003; and Worman et al, 2002). These include the riparian and hyporheic zones (Pinay et al., 2002). Understanding the role of hydrologic and biogeochemical processes through these zones will increase our capabilities to manage nitrate flux to the bay and to predict long-term nitrate loads to streams and estuaries.

1.2.2 Hyporheic Zone

The definition of the hyporheic zone varies considerably in the literature. Bencala (2000) combines definitions in suggesting that the environmental importance of the hyporheic zone is "…influence(ing) the biogeochemistry of stream ecosystems by increasing solute residence times, and more specifically solute contact with substrates, in environments with spatial gradients in dissolved oxygen and pH." Harvey and Bencala (1993) on the other hand, suggest that the hyporheic zone is a "…subsurface flow path along which water 'recently' from the stream will mix with subsurface water 'soon' to return to the stream." Recent work on hyporheic zones seeks to quantify their spatial extent through stream tracer studies (Laenen and Bencala, 2001), and to characterize the role of biogeochemical cycling within these flow paths (Jones and Holmes, 1996, Fuller and Harvey, 2000). Worman et al. (2002) describe the flow path through the hyporheic zone as a series of upwelling and downwelling events along a river reach similar to the path of a saltation load in a river channel. In this study the hyporheic zone is defined as the subsurface sediments directly below and adjacent to the streambed where groundwater and surface water are exchanged and chemically altered.

1.2.3 Riparian Zone

The riparian zone, like the hyporheic zone, is variably defined. Here it will be defined as the land spatially adjacent to a river reach. The United States Department of Agriculture (USDA) has long sought to utilize the riparian zone as a key location for nitrate reduction. The Conservation Reserve Program (CRP) and the Conservation Reserve Enhancement Program (CREP) offer incentive payments and

annual rental payments to farmers who convert riparian cropland to 'forested buffers'. While the riparian zone has the potential to remove significant nitrate, it requires a relatively high water table in order to maintain the anoxic conditions required for microbial reduction of nitrate (Burt et al., 2002).

Denitrification within the hyporheic zone is enhanced by the presence of riparian vegetation. Flora and fauna in and adjacent to stream reaches provide a reduced carbon source to streambeds. Sediment transport can bury this material, which upon decay consumes dissolved oxygen leaving anoxic microsites within the hyporheic zone. Even in locations with oxygenated surface and groundwater, this organic matter can create anoxic zones that intersect hyporheic flow paths zone (Hinkle et al., 2001).

1.2.4 Microsites of Denitrification

Koba et al., (1997) proposed that "microsites" of anoxia can develop under otherwise oxic conditions. Microsites are defined as pore spaces between particles. Denitrification is considered to occur under redox conditions between the stability fields of dissolved oxygen and reduced manganese. In a study conducted in a Japanese watershed, neither of these conditions was observed in the bulk site, however, the isotopic enrichment of ^{15}N was observed and most likely associated with the preferential bacterial selection of the lighter ^{14}N isotope during metabolism. The Japanese researchers found transport of oxygen into microsites was slow after available oxygen was utilized for microbial reduction. Conditions favorable to denitrification existed once oxygen within a microsite was consumed, yet before oxygen from the surrounding media was able to diffuse into the site. Their study was

conducted in the vadose zone, the subsurface unsaturated area above the water table.

Several other studies have measured significant rates of denitrification in otherwise

oxic conditions, which have been attributed to hyporheic denitrification (Jones and

Holmes, 1996; Fuller and Harvey, 2000; Bachman et al., 2002). The diffusion of

oxygen into water is a relatively slow process. Thus microsites would be more likely

to develop in the saturated hyporheic zone than in the riparian zone, which may have

variable water content.

1.3 Chesterville Branch

    In a National Water-Quality Assessment (NAQWA) study funded by the EPA

and performed by the United States Geological Survey (USGS), Bachman et al.

(2002) investigated the effect of hydrogeology on baseflow geochemistry in two

adjacent agricultural watersheds of Kent County Maryland (Figures 1 and 2). The

western Chesterville Branch, an agriculturally dominated sub-watershed of the

Chester River in Kent County, Maryland, is the focus of this study. The geology

(Bachman et al., 2002), hydrogeology (Focazio et al., 1998 ; Hantush and Cruz, 1999;

Bachman et al., 2002; Ator et al., 2005), and groundwater chemistry (Bohlke and

Denver, 1995; Bachman et al., 2002; Ator et al., 2005) are all relatively well

established. These published works provide a strong framework from which to

address more specific questions about the fate and transport of agricultural

contaminants.
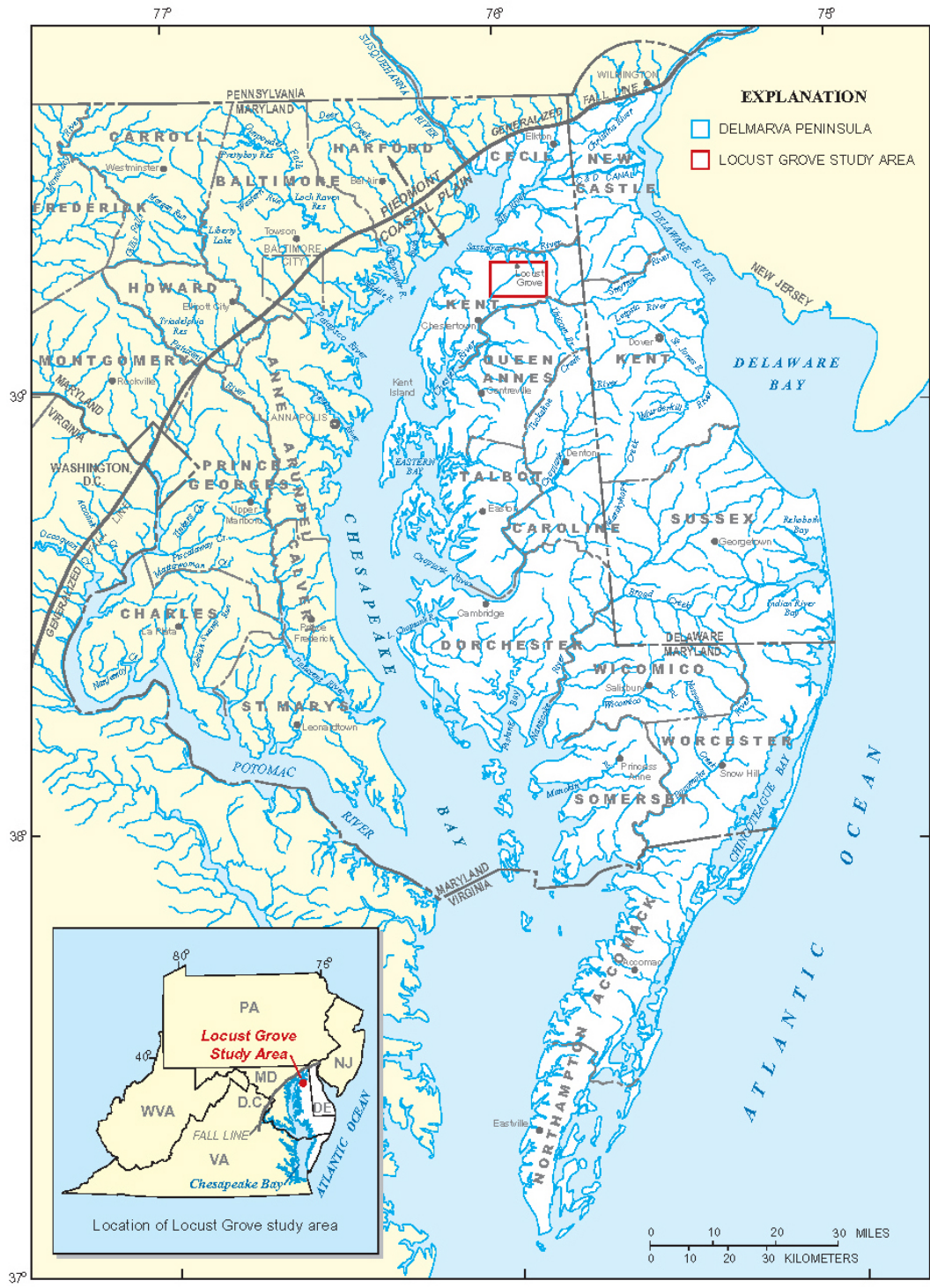
Figure 1. Map shows regional view of Locust Grove Study Site, Eastern shore of Maryland. Taken from Bachman et al. 2002.
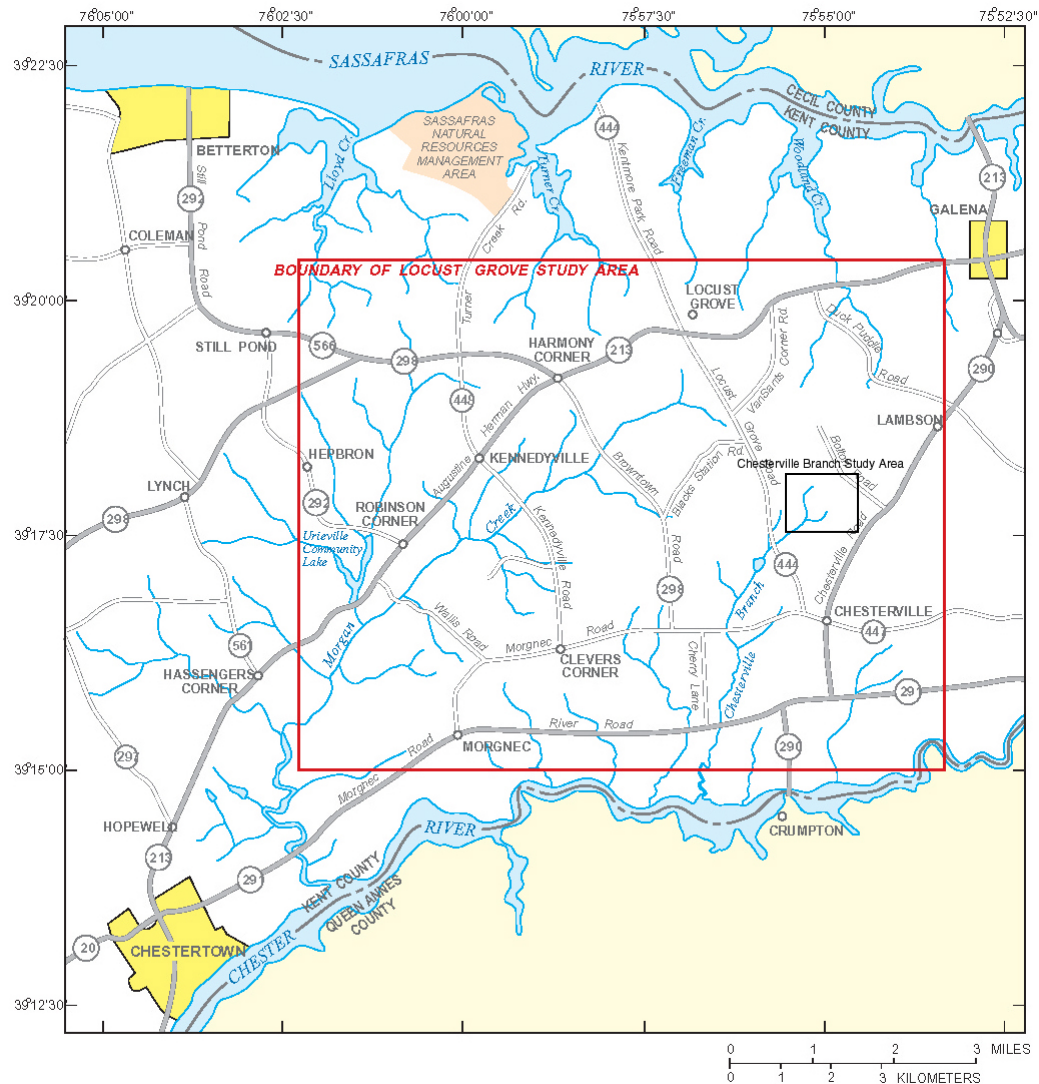
Figure 2. View of Locust Grove Study Area with Chesterville Branch Study Area outlined in black. Modified from Bachman et al. 2002.

Current models are unable to precisely predict total watershed delivery of

nutrients to bays and estuaries (Howarth et al., 1996; Smith et al., 1997; Caraco and

Cole, 1999; Preston and Brakebill, 1999; Alexander et al., 2000; Norton and Fisher,

2000; Smith et al., 2003). . The United States Geological Survey (USGS) developed

the "SPAtially Referenced Regression On Watershed" attributes (SPARROW).

Using the model USGS scientists found that the size of a stream channel increases,

the decay rate of nitrate decreases. The model accounts for various surficial

10

characteristics such as stream density, soil permeability, and temperature. These characteristics have no mechanistic link to denitrification. Conceptually a smaller channel has a higher proportion of surface water interacting with the hyporheic zone. This exchange could bring surface water in contact with anoxic conditions conducive to denitrification. In larger channels the bulk of the surface water does not exchange with adjacent soil media but rather flows downstream. While there is a loose conceptual tie, there remains many heterogeneities even among streams of the same size. Characteristics such as flow rate, channel geomorphology, groundwater character, and lithology all influence the fate of nitrate in agricultural watersheds.

The challenge to modelers is to find input parameters that are already being collected, or that can be collected using an existing infrastructure, in an inexpensive manner that will more accurately predict watershed delivery of nutrient contaminants. The accumulation of nutrients in groundwater coupled with the lag time between application and discharge, pose the greatest consistent input. This input is most influenced by parameters not included in current predictive models such as channel geomorphology, flow rate, and lithology. Understanding the dynamics between geologic character and hydrologic flow path enables better prediction nitrate flux from subsurface reservoirs

1.4 Hypothesis

The chemical characteristics of the two uppermost 1st-order tributaries of Chesterville Branch, which are both fed by groundwater springs, are considerably different. Nitrate, magnesium, and hydrogen ion concentrations decrease downstream in the ditched tributary. In contrast, the headwater sites in the unaltered tributary

have nitrate concentrations at or below detection limit, and a pulse of nitrate below the stagnant sites. This study is designed to determine the factors contributing to distinct chemical character in these adjacent 1st-order tributaries.

1. *Biogeochemical Processing of Stream Water Hypothesis:* Relatively stagnant water in the uppermost section of the unaltered tributary results in conditions of anoxia and subsequent denitrification. Nitrate concentrations then increase toward the confluence as nitrate rich groundwater discharges to the stream channel. In contrast, ditching of the other 1st-order tributary results in higher flow rates, and thus no measurable in-stream nitrate transformation.

2. *Geomorphic Hypothesis:* Physical alteration of the ditched tributary has led to higher flow rates and discharge volumes than in the unaltered tributary. The relatively incised tributary gains deeper, less anthropogenically-influenced water from the underlying surficial aquifer along its reach resulting in the 'dilution' of anthropogenic contaminants.

Chapter 2: Study Site and Approach

2.1 Previous Work and Site Description

Land use in the Chesterville branch watershed has been intensively agricultural (93%) for several decades resulting in a nitrate signature in the shallow subsurface as high as 20 mg/L (Ator et al., 2005). As shown in Figure 3, Bachman et al. (2002) found an overall downstream decrease in total dissolved nitrogen concentration in the Chesterville Branch.
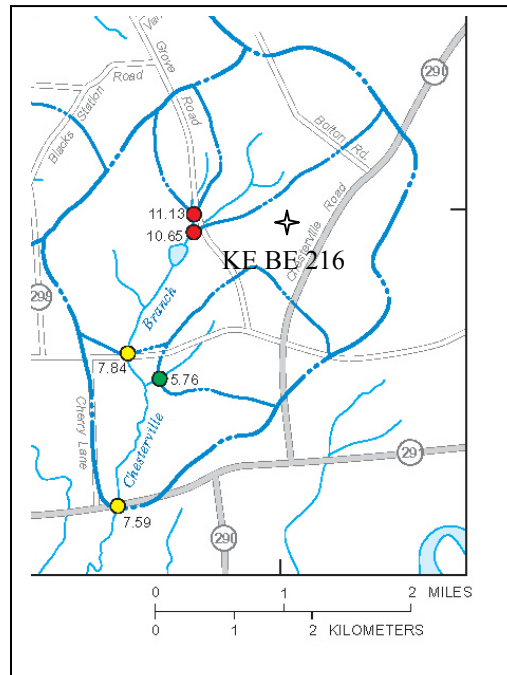
EXPLANATION

TOTAL DISSOLVED NITROGEN CONCENTRATION,
in milligrams per liter as nitrogen

- 🔴 GREATER THAN 8.3
- 🟡 5.9 - 8.3
- 🟢 3.25 - 5.8
- ⚫ LESS THAN 3.25

⬡ SUBBASIN CONTRIBUTING TO EACH STREAM-BASE-FLOW SITE

Figure 3. Total nitrogen concentration distribution in Locust Grove Study Area, April 1998 under base flow conditions. Taken from Bachman et al. 2002. Assuming all nitrogen as nitrate, dissolved nitrogen concentration of 10mg/L is equivalent to 37 mg/L nitrate.

Mass balance and mixing calculations of surface and groundwater sources, however, were insufficient to fully explain the observed trend. These authors suggest 'in-stream' or hyporheic denitrification as one possible solution.

2.1.1 Geology

Chesterville Branch is approximately 30 km from the Piedmont fall line. Here the sedimentary strata dip and thicken to the southeast. The geology of the study area was determined through the characterization and correlation of sediment cores and geophysical logs (Bachman et al., 2002). The Chesterville Branch is underlain by four geologic units. From youngest to oldest they are; (1) Holocene alluvial sediments along the axis of stream channels, (2) coarse fluvial sand and gravel of the Pensauken Formation, (3) marine sand of the Aquia Formation, and (4) marine sand and clay of the Hornerstown Formation. Below this, the Severn Formation, a regionally confining clay horizon that precludes any hydrologic communication between these and underlying strata (Bachman et al., 2002). The Old Church and Calvert formations lie between the Pensauken and Aquia formations southwest of Chesterville. The exact lateral extent of these units is not known.

Along the axis of Chesterville Branch valley is a 4-6 m thick unit of Holocene alluvium. This unit is predominantly composed of coarse sand with lenses of silt, peat, and poorly-sorted sand. Bedding within this unit is a result of recent storm erosion and subsequent deposition. Along the south flank of the study area where Chesterville Branch and Highway 444 intersect (Figure 2) the alluvial valley is 70 m wide (Bachman et al., 2002).

The Pensauken Formation, which is Upper Miocene to Lower Pliocene in age, is a large braided river system deposit with variable thickness. In the study region, well logs indicate a range between 12-15 m with an angular unconformity at its base. The unit is medium to coarse sand and gravel with lenses of silt and clay. The sand size grains are predominantly quartz with minor feldspar. The finer sediments include kaolinite, illite, and smectite (Bachman et al., 2002).

The Old Church and Calvert formations, which are Lower to Middle Miocene in age, may exist in the study area between the Pensauken and Aquia formations (Bachman et al., 2002). This unit has been documented in the region and is thought to pinch out north of the Chester River, however, it is unclear whether this unit extends into the Chesterville watershed. The Old Church Formation is a 1.5 m thick unit of fine to medium sized glauconitic sand. Glauconite forms from the digenesis of detrital biotite in reducing marine conditions (Boggs, 1995). The Calvert Formation is a compacted marine silt of low permeability. A unit similar in character was documented just southwest of Chesterville Branch in well KE BE 216 (Figure 3). This unit did not appear in the geophysical work conducted by Bachman et al. (2002).

The Upper Paleocene Aquia Formation is a coarsening-upward marine sequence with two distinct facies. The upper facies is composed of a medium quartz sand with a minimal silt-clay matrix. In the fully preserved sections, the unit is 19 m thick. Glauconite makes up 5-15% of the unit and is commonly oxidized. The lower facies, which is 9 m in thickness, is fine to medium sand with 30-50% glauconite grains in a silt-clay matrix. These glauconitic grains show no sign of oxidation. A redox transition, approximately 0.5-1 m in thickness, exists between the two

glauconitic facies. The updip limit of the Aquia Formation is just north of Highway 213 (Figure 2) (Bachman et al., 2002).

The Lower Paleocene Hornerstown Formation is also a coarsening-upward glauconitic marine sequence. The uppermost section (2-4 m in thickness) is a silt-clay facies. Below this there is a 10-13 m thick sandy section. The lower 15-16 m is comprised of a tight impermeable clay (Bachman et al., 2002).

2.1.2 Hydrogeology

There are two aquifers below Chesterville Branch, the surficial Aquia and deeper Hornerstown formations (Figure 4). Technically the surficial aquifer consists of groundwater in the Pensauken Formation (Columbia aquifer) and in the Aquia Formation. However, there is no confining unit between the two. Geophysical logs do not show a marked difference at the base of the Pensauken Formation due to the similarity in geologic character. The two aquifers are in hydrologic communication and will thus be referred to as a single unconfined surficial aquifer, the Aquia.

A low permeability clay-rich unit at the base of the Aquia aquifer results in a sharp gamma spike in geophysical logs (Bachman et al., 2002). Geophysical waves travel more quickly through dense material. When a seismic wave travels through this unit its speed increases due to the dense and tightly packed clay. However, there is disagreement in the literature about the degree to which the unit is confining. Some authors suggest it is fully confining (Dunkle et al., 1993; Reilly et al., 1994) while others indicate it is only partially-confining (Bohlke and Denver, 1995; Bachman et al., 2002). Cores drilled in the study region show a 3.8 m interval of tight and nearly dry clay (Bachman et al., 2002). This, in addition to the distinct chemical character

of water above and below the aquaclude, makes a convincing argument for this being

a regionally confining unit. The Hornerstown aquifer located below the aquaclude is

9-10 m thick. It is underlain by a confining unit 10-15 m thick (Bachman et al.,

2002).

Bohlke and Denver (1995) used tritium (H^3) and chlorofluorocarbon

concentrations (CCl_2F_2 specifically) to calculate the age of groundwater below

Chesterville Branch. They found recharge dates ranging from pre-1940 to 1980 in the

surficial Aquia aquifer. Water discharging from second-order reaches was on the

order of 20+ years old (uncertainties ranging between $\pm$ 5-10%). Water levels

measured from in-stream wells were consistently above stream level, indicating a

strong vertical hydraulic gradient. In one particular location, at the intersection of

Chesterville Branch and Route 444 (Figure 3), the samples at the edges of the stream

channel were ~10 years younger than samples taken from the center of the channel.

This infers a strong convergence and vertical upwelling of water with variable flow

paths.
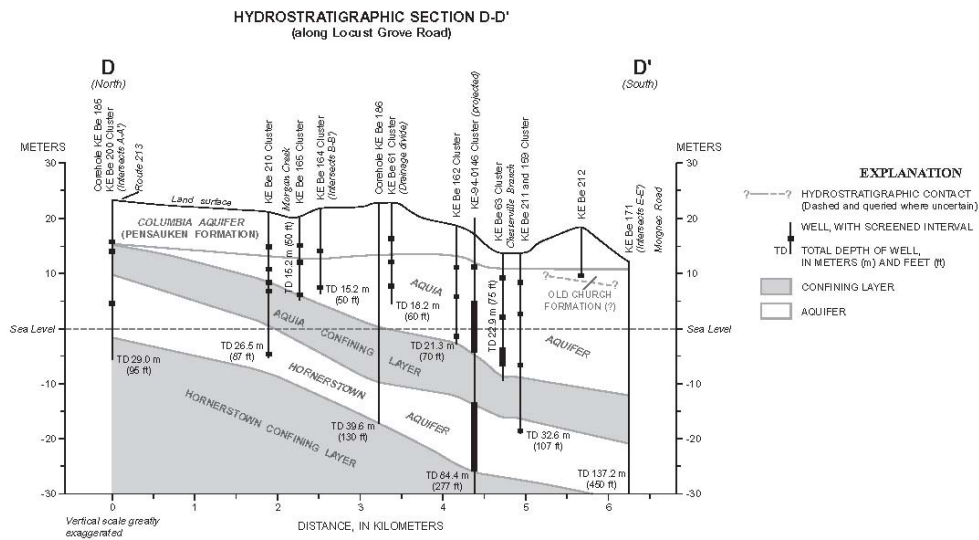
Figure 4. Hydrogeologic cross-section taken from Bachman et al. (2002). The Aquia aquifer is the sole influence to the study site. Deeper Hornerstown groundwater does not discharge in the 1st-order tributaries (Bohlke and Denver, 1995)

2.1.3. Groundwater Chemistry

Bohlke and Denver (1995) identified three types of groundwater based on chemical characteristics; oxic, suboxic, and anoxic. Oxic water is defined as having dissolved oxygen concentration greater than 5 mg/L, and nitrate concentration greater than 3 mg/L, with a residence time less than 25 years. Anoxic water is defined as having nitrate concentration at or below detection limit (0.05 mg/L) and no measurable dissolved oxygen. Deeper in the Aquia, near the redox transition, a third type of water was identified. These authors interpreted this deeper water to be a mixture of Hornerstown and Aquia waters, and referred to this reservoir as suboxic. This suboxic water still exhibits agricultural influence; nitrate concentrations range between 2-3 mg/L, dissolved oxygen concentrations are greater than 5 mg/L, and a recharge date earlier than 1970 has been indicated. Only two suboxic sampling sites

18

were documented however, and both were downstream of Route 444 (Figure 3), which is outside the study area of this project. In contrast, the core log observations and the chemical character of the suboxic water suggests a limited degree of hydrologic communication between the Aquia and Hornerstown aquifers (Bohlke and Denver, 1995).

Bohlke and Denver (1995) also observed variability in nitrate concentrations within the surficial aquifer. Based on their dating techniques nitrate systematically decreased with increasing age. This observation was interpreted as being related to increasing agricultural application of fertilizer with time. Magnesium in the aquifer and streams is predominantly derived from dissolution of crushed dolomite to agricultural fields. In the Locust Grove Site, magnesium concentration, like nitrate, systematically decreased with increasing age.

Dissolved gas concentrations near the redox transition in the lower Aquia aquifer suggest that nitrate concentrations there are not attributable to denitrification. Despite low dissolved oxygen concentrations, there is no excess of nitrogen gas. In the case of significant denitrification, nitrate reduction would produce an excess of nitrogen gas. This observation suggests that the relatively lower nitrate concentrations in the pre-1970 recharge waters are a result of lower fertilizer application rates rather than denitrification. This is confirmed by systematic variation of other agricultural contaminants such as magnesium. Mineralogical characterization of the redox transition suggests that the electron donor for denitrification would most-likely have been an iron sulfide mineral. Beneath Chesterville Branch, the redox transition occurs at a depth of roughly 50 meters. At

19

this depth reduced organic matter is not a component of the lithology. Thus,

denitrification utilizing an iron sulfide mineral would result not only in excess

nitrogen gas, but also elevated sulfate concentrations, neither of which are observed.

The nitrogen and argon gas concentrations in the oxic Aquia aquifer are consistent

with water equilibrated with the atmosphere. Gas measurements of the anoxic

Hornerstown aquifer, however, indicate an excess of N_2 when normalized to argon.

Mass balance calculations indicate nitrate concentrations prior to denitrification were

1-2 mg/L in the Hornerstown aquifer (Bohlke and Denver, 1995).

A basic mixing equation was used by Bachman et al. (2002) to estimate

groundwater discharge. Notably, mixing equation calculations were unable to

account for decreasing nitrate concentrations in Chesterville Branch (Figure 3). Even

by assigning groundwater an average nitrate concentration of 0 mg/L, the calculated

nitrate concentration remains higher than measured. This suggests an alternative in-

stream process for the removal of nitrate, such as hyporheic denitrification.

2.1.4. Site Description

Chesterville Branch, located in Kent County, Maryland (Figure 1), is a sub-

watershed of the Chester River and the Chesapeake Bay. Chesterville Branch is

dominated by agricultural land use. Currently 21% of the Chesterville Branch

watershed is cultivated nursery, 72% is cultivated corn and soy, and the remaining

7% is riparian vegetation that occurs in narrow bands adjacent to stream channels

(Bachman et al., 2002; Ator et al., 2005). The site includes two 1st-order tributaries

(each has ~1km^2 drainage area) and a small reach after their confluence. The

geomorphology of the eastern tributary suggests an unaltered stream channel, and is

referred to as the 'unaltered tributary'. In contrast, the western tributary has been

ditched to enhance drainage from surrounding fields, and is referred to as the 'ditched

tributary' (Figure 5). The second-order stream they combine to form is referred to as

the 'main stem' (Figure 6).

Surface water samples were taken for each sampling date at 25 m to 50 m

increments (Figure 7). The unaltered tributary was sampled from 100 m above the

confluence, ditched tributary 300 m from confluence, and the main stem to 150 m

downstream of the confluence. Samples were taken at base-flow conditions

beginning in November 2003 through October 2004. Base flow is defined as the

groundwater contribution to a stream (Fetter, 1994). Sampling dates are shown in

Table 1.

Table 1. Sampling dates. * Samples taken on June 5 were only used for temporal variation characterization..

November 26, 2003
June 5, 2004*
July 1, 2004
July 21, 2004
August 10, 2004
October 29, 2004

Figure 5. Above is a picture of the ditched tributary. Algae and plant material is growing in the channel. The elevation drop between the base of the stream bed and the surrounding field is roughly 1.5 meters. The image below is of the unaltered tributary. The width of the channel is substantially smaller than the ditched channel and the depth of the channel is less than 0.25 meters.

Figure 6.   The main stem at sample site MS-100 looking downstream. Relief from streambed to banks is roughly 0.5 meters.
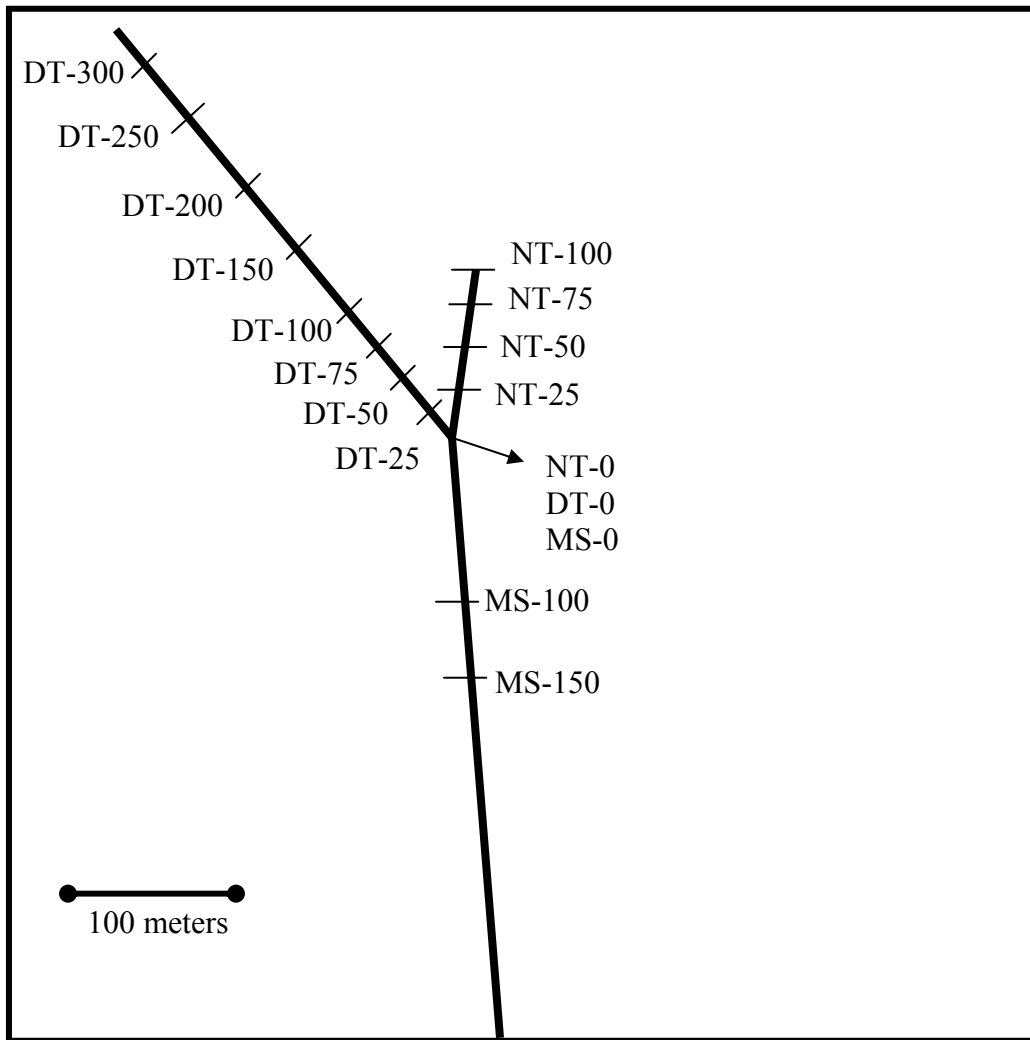
Figure 7. Schematic of sampling sites in Chesterville Branch.

2.2 Field Approach

2.2.1 Field Procedures

Sites were established using a metric measuring tape and flagged for consistency. As shown on Figure 7, the zero datum is defined as the confluence between the ditched and unaltered tributaries. Sites downstream of this are recorded as positive distance values, and sites upstream of this in each of the tributaries are negative distance values. Distance values are certain to at least ± 1 meter.

24

Since sampling required standing in the stream channel, the schedule began at the furthest downstream point, site MS-150. Starting downstream and working toward the headwaters ensured samples were undisturbed by sediment stirred up while standing in the channel. The unaltered tributary was sampled before the ditched tributary. The entire sampling cycle was complete within 4 hours. Field parameters (temperature, and pH) were obtained in-situ using a HACH ion probe. The pH meter was calibrated using standard reagents with pH values of 4.01, 7.00, and 10.01. The meter automatically generates a calibration curve and adjusts for temperature variations. External reproducibility measurements, however, yield a 1σ uncertainty of $\pm$ 1.1%. There is no calibration for temperature. External reproducibility measurements yielded a 1σ uncertainty of $\pm$ 0.3%. All samples were collected in High Density Plastic Ethylene (HDPE) bottles that were acid washed and triple rinsed with deionized water. Samples were taken from the center of the water column at each sample site.

Samples collected on November 26th were filtered in the field through a 0.45-μicron filter using a stainless steel filter stand and peristaltic pump. Filtered samples were collected in duplicate in 125 mL bottles. Samples were transported to the laboratory in a cooler of ice and refrigerated upon arrival. Alkalinity was not measured on this sampling date and can not be measured retroactively due to the distributed equilibrium of filtered samples by atmospheric exchange with carbon dioxide.

All other samples were collected in 125 mL duplicates. Samples were transported to the laboratory in a cooler of ice and refrigerated upon arrival. These

samples were filtered in the lab less than 24 hours after collection. The laboratory

filtration is discussed in the laboratory methods section. An additional 125 mL was

taken for alkalinity titration.

Macro algae growing in the stream was collected on August 10th and October

29th for carbon and nitrogen isotopic analysis. Algae samples were stored in plastic

bags in a cooler. Once at the laboratory, all samples were frozen.

Dissolved inorganic carbon (DIC) isotopic analysis used water from the 125

mL duplicates except for October 29th sample date. Samples collected on October

29th were taken in 15 mL HDPE bottles. Bottles were sealed below the surface of the

water without headspace to prevent exchange with atmospheric gases.

Flow measurements were attempted using a Swoffer digital flow meter. The

low velocity and small channel size however were at the lower end of instrument

capabilities. A further complication to flow measurement was the presence of

abundant algae and other plant material growing in the channel, which obstructed the

movement of the propeller, and semi-solid stream bed. Channel dimensions were

also obscured by the presence of plants. All of these factors contributed to the

inability to accurately measure stream flow at the study site. As a consequence,

various chemical parameters have been used to quantify the relative contributions of

the unaltered tributary and ditched tributary. In addition, temporal variations in base

flow are related to the adjacent Morgan Creek flow conditions, which has a USGS

gauging station.

2.3 Laboratory Approach

2.3.1 Filtration

Samples taken from dates on and after July 1st were filtered in the lab. Each 250 mL sample was filtered through a 0.22-µm membrane filter within 24 hours of collection to remove particulate matter and micro-organisms. This prevents further bacterial chemical alteration of samples. Samples were run through a 500 mL Nalgene double chamber filter using lab vacuum. The chamber was triple rinsed with deionized water between samples. These samples were then refrigerated and used for major ion analysis.

2.3.2 Alkalinity

Alkalinity is defined as the ability of a solution to neutralize $[H^+]$ and is measured as:

$$Alk = [OH^-] + [HCO_3^-] + 2[CO_3^{2-}] - [H^+] \qquad (6)$$

Alkalinity was measured on unfiltered samples using a HACH digital titrator. 100 mL of unfiltered sample was put into a glass beaker and phenolphthalein indicator was added and the solution stirred. If the solution turned pink, it would then be titrated to a colorless endpoint using 0.1600 ± 0.0001 M H_2SO_4. Phenolphthalein indicator appears pink at pH values above 8.3, and returns to a colorless state below this value. The pH of 8.3 is significant insofar as that is where concentrations of HCO_3^- and CO_3^{2-} are equal. None of the samples measured in this study turned pink at this step as is expected based on field pH measurements. This confirms that no significant portion of alkalinity was in the form of OH^- or CO_3^{2-}.

Next a bromcresol green-methyl red indicator powder packet was added to the beaker. The solution turns some color of green or blue, after which 0.1600 ± 0.0001 M H_2SO_4 is used to titrate to a light pink endpoint of 4.5. At this pH, all of the HCO_3^- has been neutralized. The amount of acid required is proportional to the amount of alkalinity present. The volume and titrating acid concentrations described above are those used for alkalinity values between 10-40 mg/L. A few samples were out of this range requiring a 1:4 dilution followed by the same steps. All alkalinity measurements given are equivalent to total bicarbonate in this study due to the absence of significant hydroxide or carbonate alkalinity. External reproducibility measurements yield a 1σ uncertainty of $\pm 4.4\%$.

2.3.3 Cation Analysis

Calcium, magnesium, and sodium concentrations were measured for each sample using a Perkin Elmer model 2380 flame atomic absorption spectrophotometer (AAS). In this method a liquid sample was aspirated into an acetylene-air flame. Each element has a corresponding lamp that produces a characteristic beam of radiation for the element to be analyzed. The radiation from the lamp is passed through the flame to a detector. The attenuation of the beam in the flame, relative to the standard, is related to the concentration of the element to be analyzed. Standards were made using calibrated glassware and 1000 ppm standards for calcium, magnesium, and sodium. The instrument is rated for a linear range, which varies by metal of interest. Samples required dilution in order to fall within this range. Table 2 lists the linear range, dilution, 1σ uncertainty, and prepared standard concentrations for each metal analyzed.

Table 2. Flame Atomic Absorption parameters

Metal	Linear Range	1σ	Dilution	Prepared Standards (mg/L)
Calcium	0-5 mg/L	± 1.1%	1:9	0.1, 1, 3, 5
Magnesium	0-0.5 mg/L	± 2.2%	1:21	0.05, 0.1, 0.3, 0.5
Sodium	0-1 mg/L	± 3.6%	1:21	0.1, 0.5, 0.7, 1.0

2.3.4 Anion Analysis

Nitrate concentrations were determined using a Technicon AutoAnalyzer II ion chromatograph and NAP software/channel #3/ XYZ sampler. Lois Lane of Horn Point Laboratory, University of Maryland, performed the analysis. Filtered samples are passed through a granulated copper-cadmium column to quantitatively reduce nitrate to nitrite. Total nitrite concentration was then determined by diazotizing with sulfanilamide and coupling with N-1-naphthylethylenediamine dihydrochloride to form a colored azo dye. Nitrate concentration is obtained by subtracting the initial nitrite value from the nitrite plus nitrate concentrations. Nitrate concentrations were either diluted in order to fall within the high range method (10-400 µM) or analyzed using the low nitrate method (0-10 µM). The relative 1σ uncertainties for the high and low range methods are ± 3.2% and ± 0.17% respectively.

2.3.5 Isotopic Analysis

Carbon isotopes of dissolved inorganic carbon (DIC) were analyzed using a Multiflow headspace inlet and Micromass (GV) Isoprime gas source mass spectrometer. Vials were prepared by delivering 500 µL of an 85% phosphoric acid solution. After being capped, the vials were flushed for 90 seconds with inert helium to remove atmospheric gases from the headspace. 1 mL of sample was then delivered

through the septum of each vial with a syringe. The syringe was triple rinsed with

each sample prior to delivery. The phosphoric acid drives the speciation of the

dissolved inorganic carbon toward CO_2 by lowering pH to values well below the first

acidity constant of 6.3. An equilibration time of 12 hours at 40° Celsius allows for the

DIC species to equilibrate, forming dissolved CO_2, and ultimately exsolve into the

headspace. The partial pressure of CO_2 in the headspace at the instant the sample is

injected is equal to zero. This resulted in a high proportion of DIC exsolving into the

head space, minimizing fractionation at this step (after Nascimento et al., 1997). A

laboratory carbonate sample was used to calibrate seawater, which was used as a DIC

standard. Seawater standards were prepared as described above. 200 µg of the solid

carbonate standard was placed into a vial and flushed for 90 seconds with inert

helium. Then 500 µL of an 85% phosphoric acid solution was delivered to the vials

through the septum using a syringe. The headspace was then analyzed after a five

minute equilibration time in the heated sample tray. The 1σ uncertainty of DIC

isotopic measurements is $\pm\ 6.6\%$.

Algae samples were rinsed with deionized water to remove dirt or organisms.

Samples were then freeze-dried using a Labconco Freezone 4.5. Dry samples were

ground to a powder with a mortar and pestle. Approximately 200 µg of powdered

algae was placed into tin capsules, which were then folded and sealed. The samples

were passed through a Eurovector elemental analyzer (EA) coupled to a Micromass

continuous flow gas source mass spectrometer in a stream of helium carrier gas. The

samples were combusted in the EA at a temperature of $1020\ ^{0}C$. The resulting CO_2

and N_2 gases are passed through a water trap and a C/N gas chromatography column

to further purify and separate the species prior to their introduction into the source of the mass spectrometer. Both nitrogen and carbon isotope values were obtained. A house standard urea was used for calibration of C/N as well as δ^{13}C and δ^{15}N compositions. The Urea standard was used to establish uncertainty for individual sample runs. The average 1σ uncertainty was $\pm$ 0.23% and $\pm$ 1.5% for carbon and nitrogen isotopes respectively.

Chapter 3: Results

It is proposed that groundwater discharging to each of the tributaries follows different flow paths. In this hypothesis physical alteration of the ditched tributary results in access of deeper, more dilute groundwater (Figure 8), thus nitrate, calcium, magnesium, and hydrogen ion concentration should be decreasing along this reach based on the known stratigraphic and chemical characteristics of the Aquia aquifer (Bolhke and Denver, 1995; Bachman et al., 2002). It is not clear, however, whether there is also a gradient in DIC isotopic composition in the surficial Aquia aquifer. On the other hand, groundwater discharging in the unaltered tributary should be of similar age and chemical composition (Figure 9). The stagnant upper section of the unaltered tributary is anoxic due to the consumption of dissolved oxygen by decaying plant material. This results in in-situ denitrification. Thus nitrate concentrations in the upper section will be considerably lower than elsewhere in the study site. Corresponding to this decrease in nitrate, an increase in alkalinity is expected downstream. The proposed electron donor for denitrification is reduced carbon in the stream channel. This is confirmed by excess bicarbonate at the stagnant sites.

A table of results is presented in Appendix A.
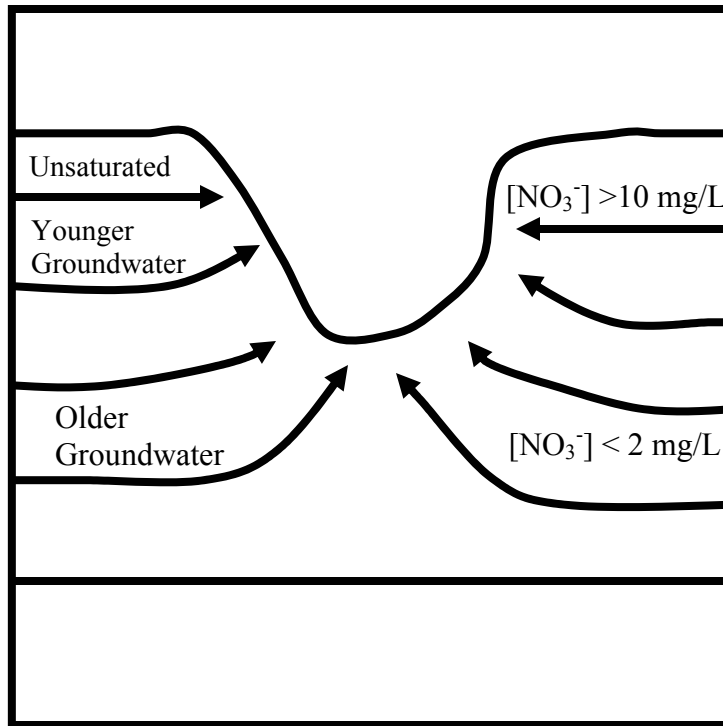
Figure 8.   Schematic of groundwater discharging to the ditched tributary.
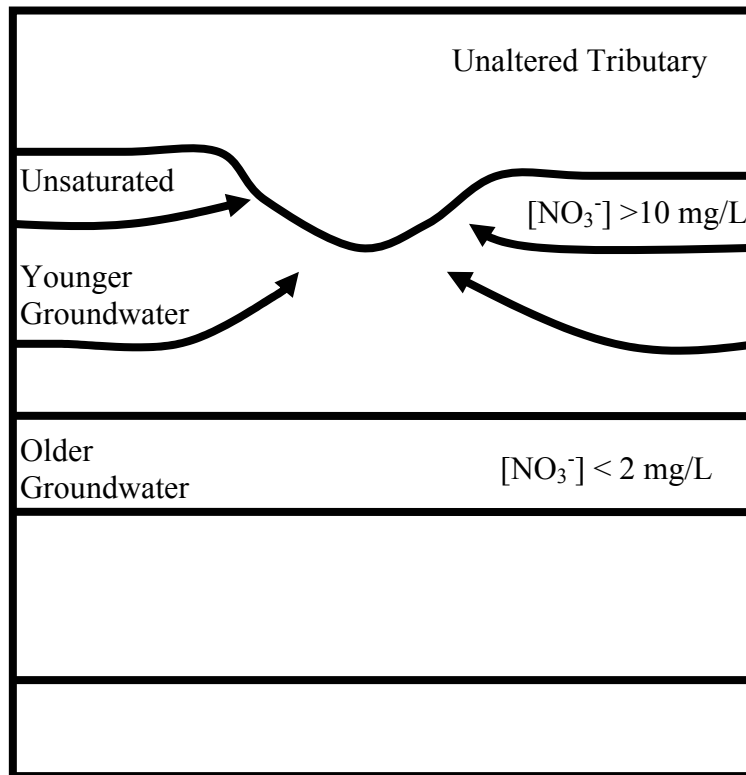
Figure 9.   Schematic depicting groundwater discharge to the unaltered tributary.

3.1 Field Measurements

3.1.1 pH

Field pH measurements are shown graphically for each sample date in Figure 10. On each sampling date, pH increased along the ditched tributary and decreased along the unaltered tributary. Measured pH values in the uppermost sites of the unaltered tributary are higher than any in the ditched tributary. On November 26th, the pH remains higher than any measured in the ditched tributary. On all other sample dates pH in the unaltered tributary drops below the values measured on the ditched tributary nearer their confluence.

Temporal variations were analyzed by averaging all values along the ditched tributary, natural tributary, and main stem for each sample date. This type of average will be referred to as 'whole site' average throughout the results and discussion sections. These variations are shown in Figure 11. The unaltered tributary averages tend to be higher than ditched tributary averages. On October 29th however this trend was reversed with the ditched tributary being the most basic, and unaltered tributary most acidic. However this date also exhibits the least variation in pH. In contrast, the earliest sample date exhibits the largest pH variation. Average pH values are the most acidic on July 1st and November 26th.
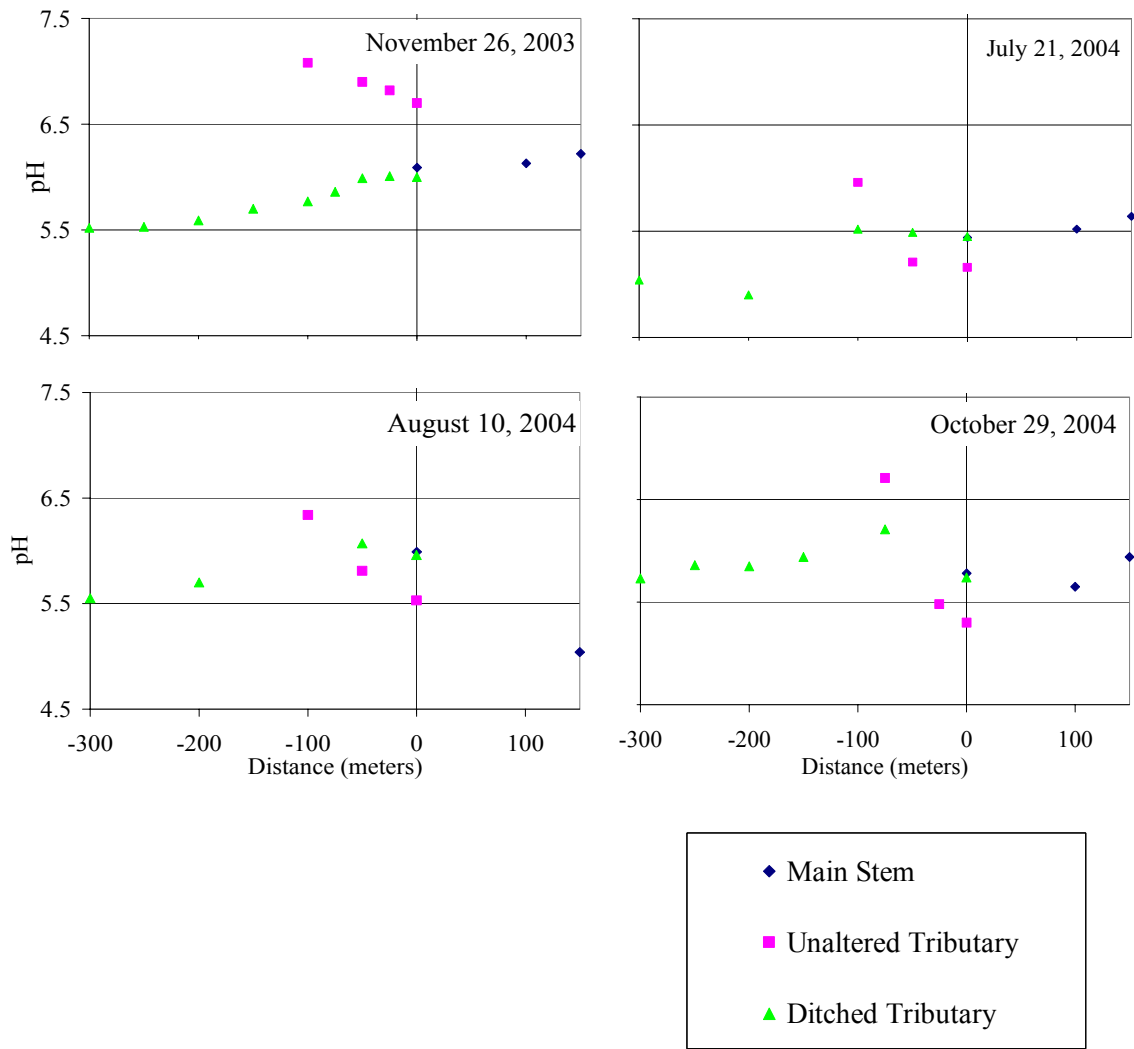
Figure 10. Spatial variation in pH for each sample date. The 1-σ uncertainty in pH measurements is ± 1.1%. Uncertainty is smaller than the symbol used.
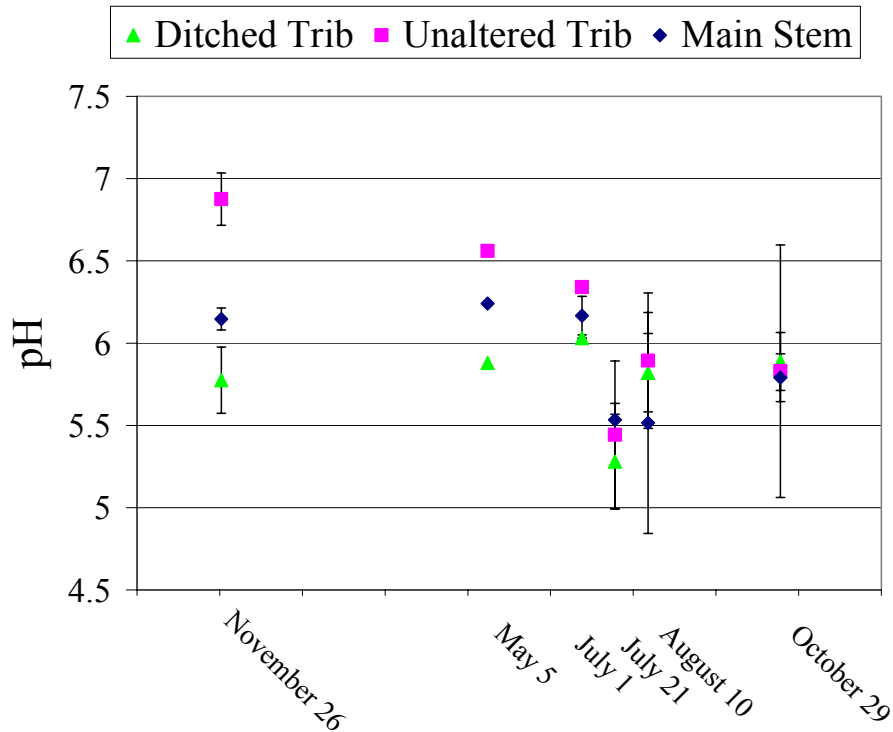
Figure 11. Temporal variation in pH. Each point represents the average of all values obtained along a given reach on a given sample date. Error bars show the standard deviation of values on a given sample date. On sample date May 5th measurements were made on only at the confluence and thus there is no data set to calculate standard deviation.

3.1.2 Temperature

Field temperature measurements are shown graphically for each sample date in Figure 12. The temperature values reflect seasonal temperature changes. In general there is little variation on each sampling date except for in the unaltered tributary on November 26th, July 21st, and August 10th. This is a result of the relatively smaller size of the unaltered tributary. On November 26th, the colder temperatures result from the smaller tributary being more efficiently cooled by the air. On August 10th and July 21st, the unaltered tributary cools substantially from the headwaters to the confluence. The stagnant upper reaches are warmed through

36

interaction with warm summer air temperatures. Previous studies suggest discharging

groundwater along the entire reach (Bohlke and Denver, 1995; Bachman et al., 2002).

This incoming water mixes with the water upstream resulting in a cooling trend

toward the confluence.

Figure 13 shows the whole site average temporal variation in temperature.

The coldest sampling dates coincide with winter months, and the warmest sampling

dates coincide with summer months. Notably, November 26th and July 21st exhibit

the greatest variation in temperature. The general variation can be attributed to the

relative channel size. The smaller unaltered tributary is more effectively cooled and

heated than the larger ditched tributary and main stem.
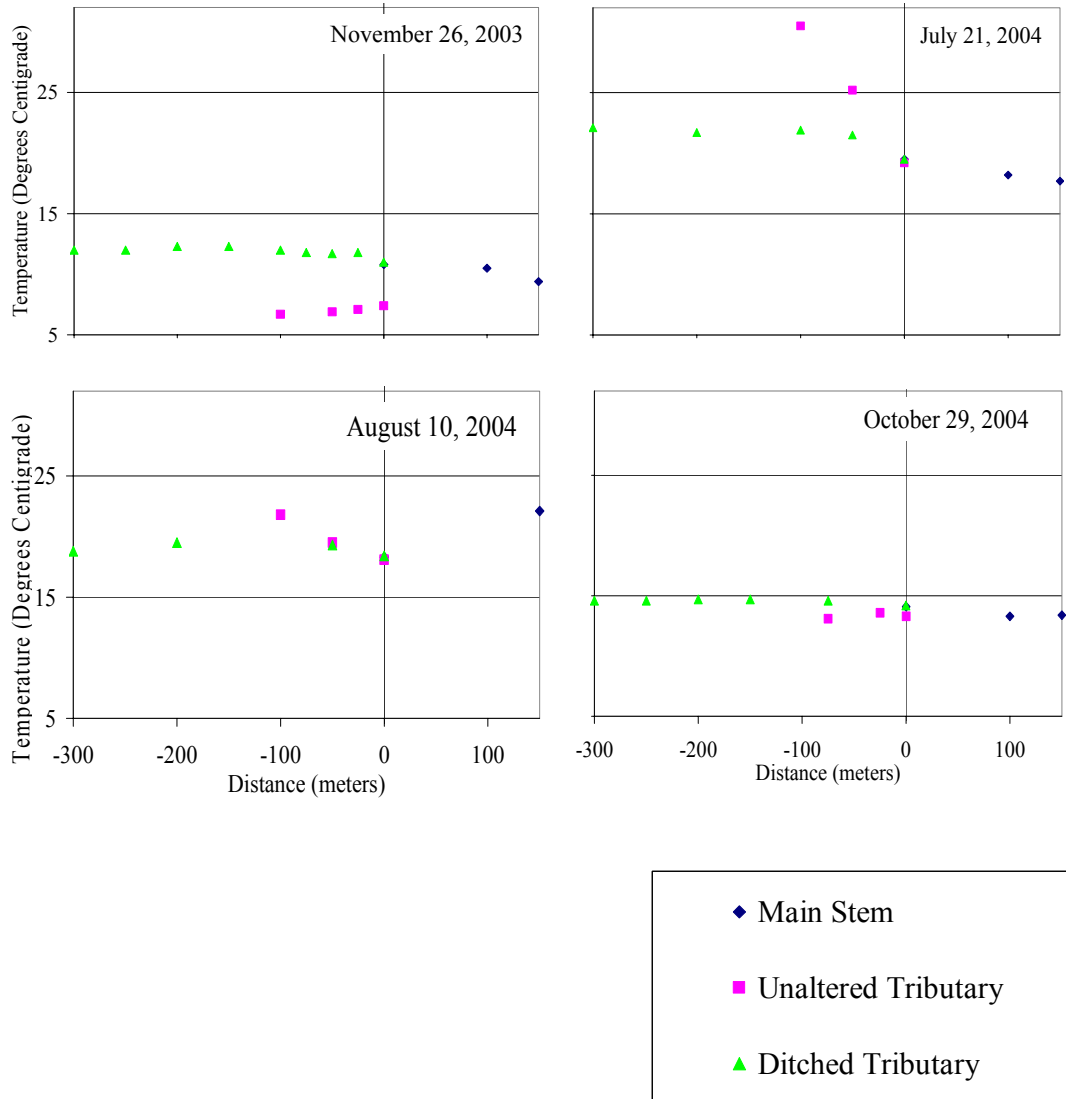
Figure 12. Spatial variation in temperature for each sample date. Uncertainty in temperature is ± 0.25%, smaller than the symbol used.

Figure 13. Temporal variation in temperature. Each point represents the average of all value obtained along a given reach on a given sample date. Error bars show the standard deviation of values on a given sample date. On sample date May 5th measurements were only made on all three sections at the confluence and thus there is no data set to calculate standard deviation.

3.2 Laboratory Results

3.2.1 Alkalinity

Alkalinity measurements are shown graphically for each sample date in Figures 14. Based on the pH driven speciation of dissolved inorganic carbon, alkalinity in this study is equivalent to bicarbonate concentration. Sampling dates July 21st, August 10th, and October 29th have decreasing alkalinity along the unaltered tributary and increasing alkalinity along the ditched tributary. The correlation of

decreasing alkalinity with distance has an average r^2 value of 0.84 (n=3) and 0.76 (n=3) for the unaltered and ditched tributary, respectively. In contrast, the trends for July 1st slightly increase along the unaltered natural tributary and slightly decrease along the ditched.

Whole stream average temporal variations of alkalinity are shown in Figure 15. Alkalinity in the unaltered tributary is consistently highest of the three stream reaches. Aside from July 1st, the ditched tributary exhibits the lowest values. There is no temporal trend to the alkalinity measurements. The main stem values are relatively closer to the ditched tributary values than unaltered tributary values. This confirms that the ditched tributary volumetrically contributes relatively more alkalinity than the natural tributary to the main stem.
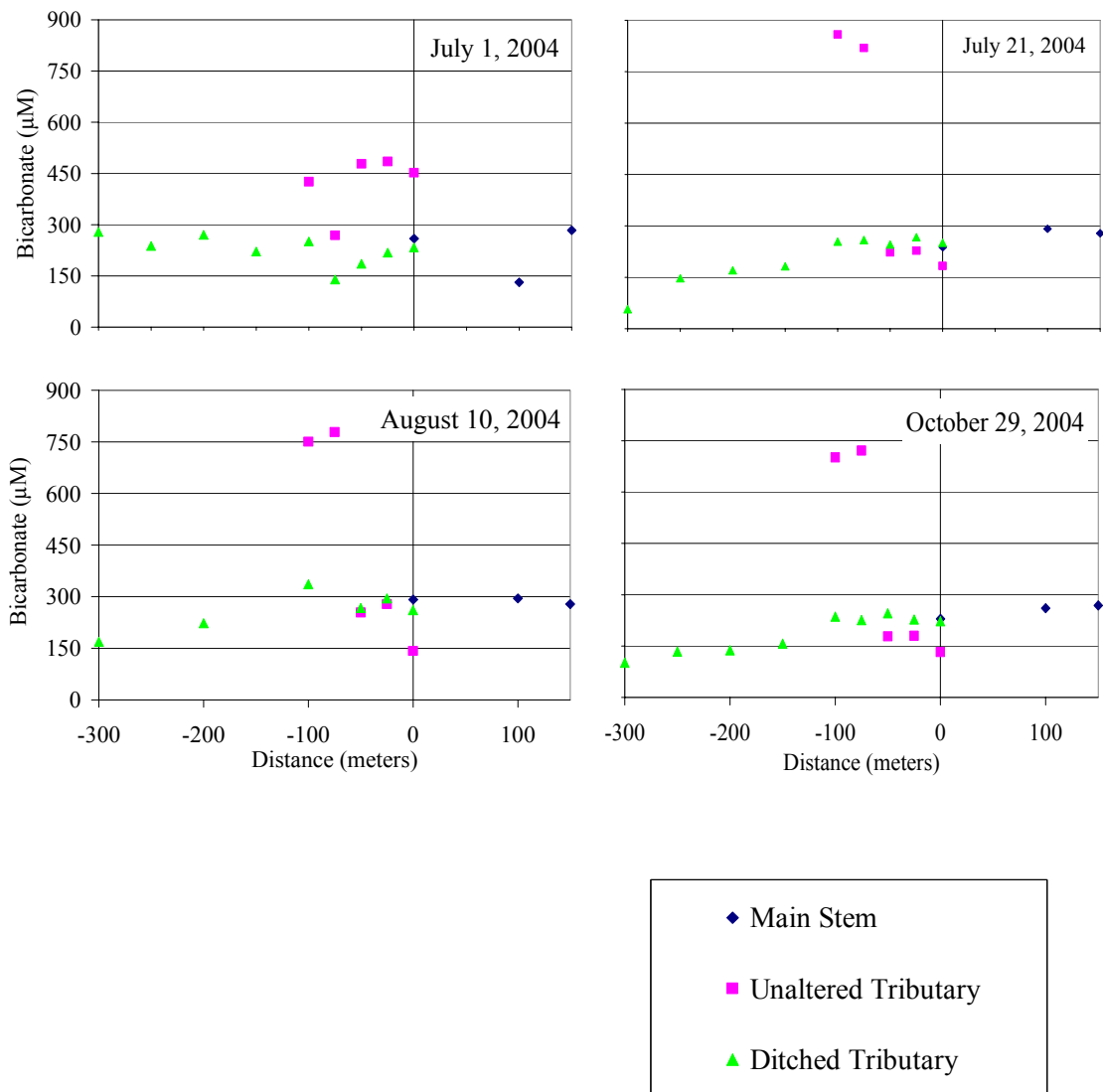
Figure 14. Spatial variation in bicarbonate concentration. Uncertainty in bicarbonate measurement is ± 4.4%, smaller than the symbol used.

Figure 15.   Temporal variation in alkalinity. Each point represents the average of all value obtained along a given reach on a given sample date. Error bars show the standard deviation of values on a given sample date. On sample date May 5th measurements were only made on all three sections at the confluence and thus there is no data set to calculate standard deviation.

3.2.2 Calcium and Magnesium

Calcium in this system has two possible sources, dissolution of sedimentary limestone in underlying strata or dissolution of crushed dolomite used on agricultural fields (Bohlke and Denver, 1995). A higher concentration may result from either of these factors. Limestone has a calcium to magnesium ratio equal to infinity, and dolomite has a calcium to magnesium ratio of one.

Calcium measurements are shown graphically for each sample date in Figure 16. Calcium concentrations consistently decrease along the unaltered tributary. Concentrations slightly increase in the ditched tributary at all sample dates other than

November 26th. Whole site averaged temporal variations are shown in Figure 19.
Sampling date November 26th exhibits the highest degree of variability; July 21st
exhibits the least. Generally, calcium concentrations are lowest in the summer
months.

Magnesium measurements are shown graphically for each sample date in
Figure 17. Magnesium concentrations increased in the unaltered tributary in all
sample dates except November 26th. Sample sites NT-50 and NT-25 exhibit
anomalously high magnesium concentrations on all sample dates except July 1st.
Magnesium concentrations decreased in the ditched tributary on all sample dates
except July 1st. Whole site averaged temporal variations are shown in Figure 20. The
highest variation in concentration was on November 26th, the least variation on July
21st. Generally magnesium concentrations are lowest in the summer months.

The molar ratio between calcium and magnesium is shown in Figure 18. On
each sampling date the molar ratio increased in the ditched tributary and decreased in
the unaltered tributary. Whole site averaged temporal variations are shown in Figure
21. There is no appreciable trend in this data.
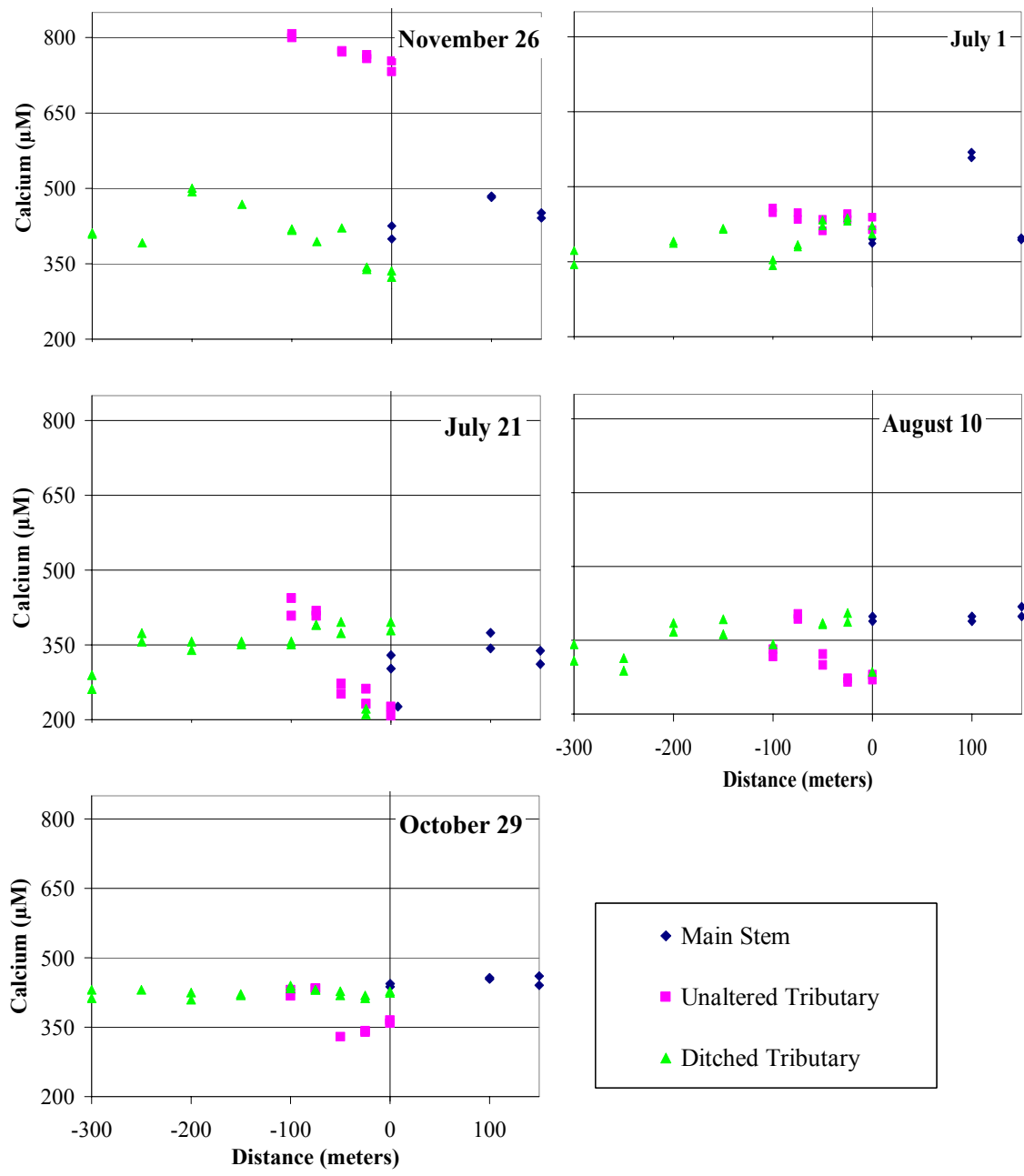
Figure 16. Spatial variation in calcium for each sample date. Uncertainty is ± 1.1%, smaller than the symbol used.
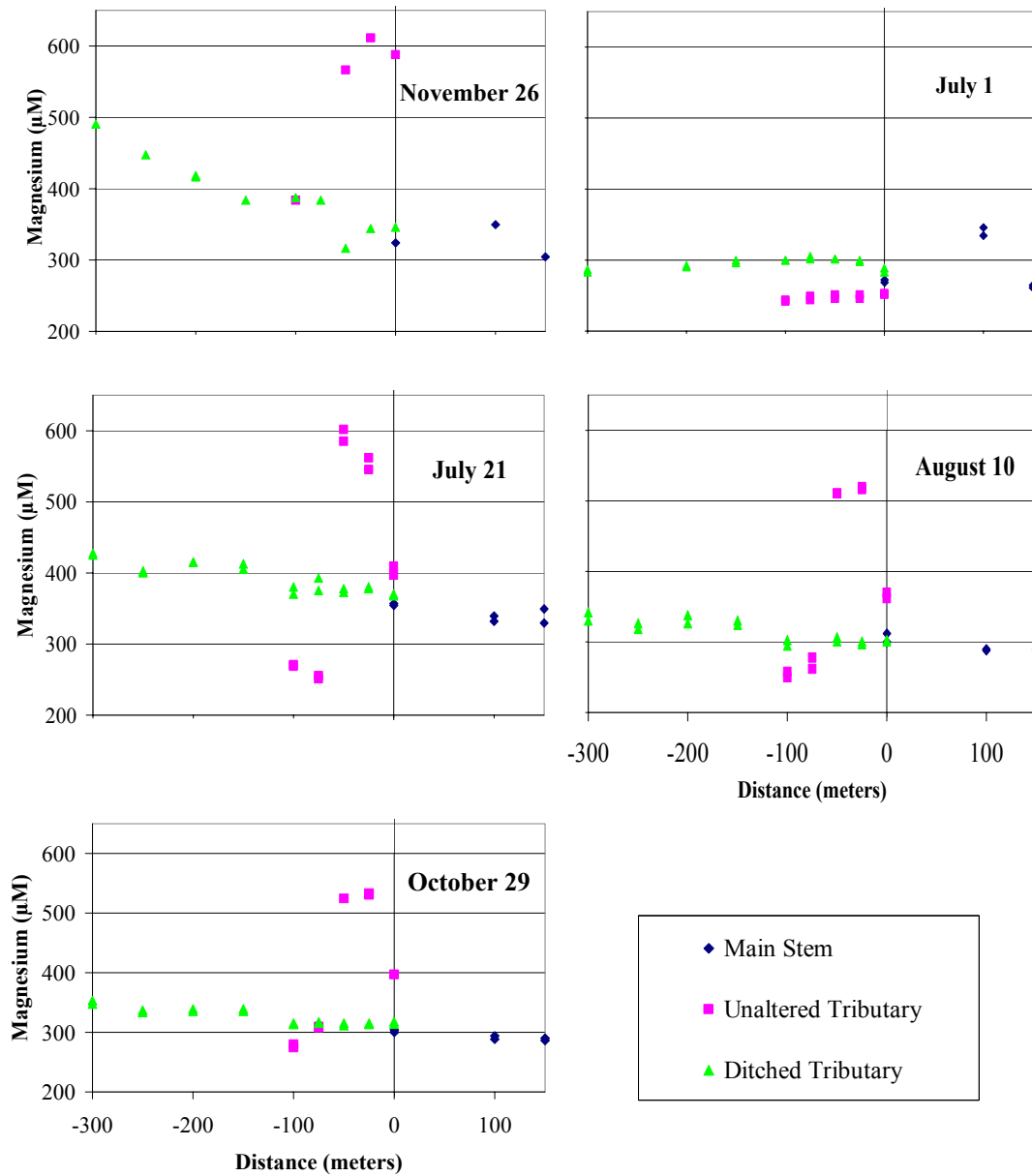
Figure 17. Spatial variation in magnesium concentration. Uncertainty is ± 2.2%, smaller than the symbol used.

45
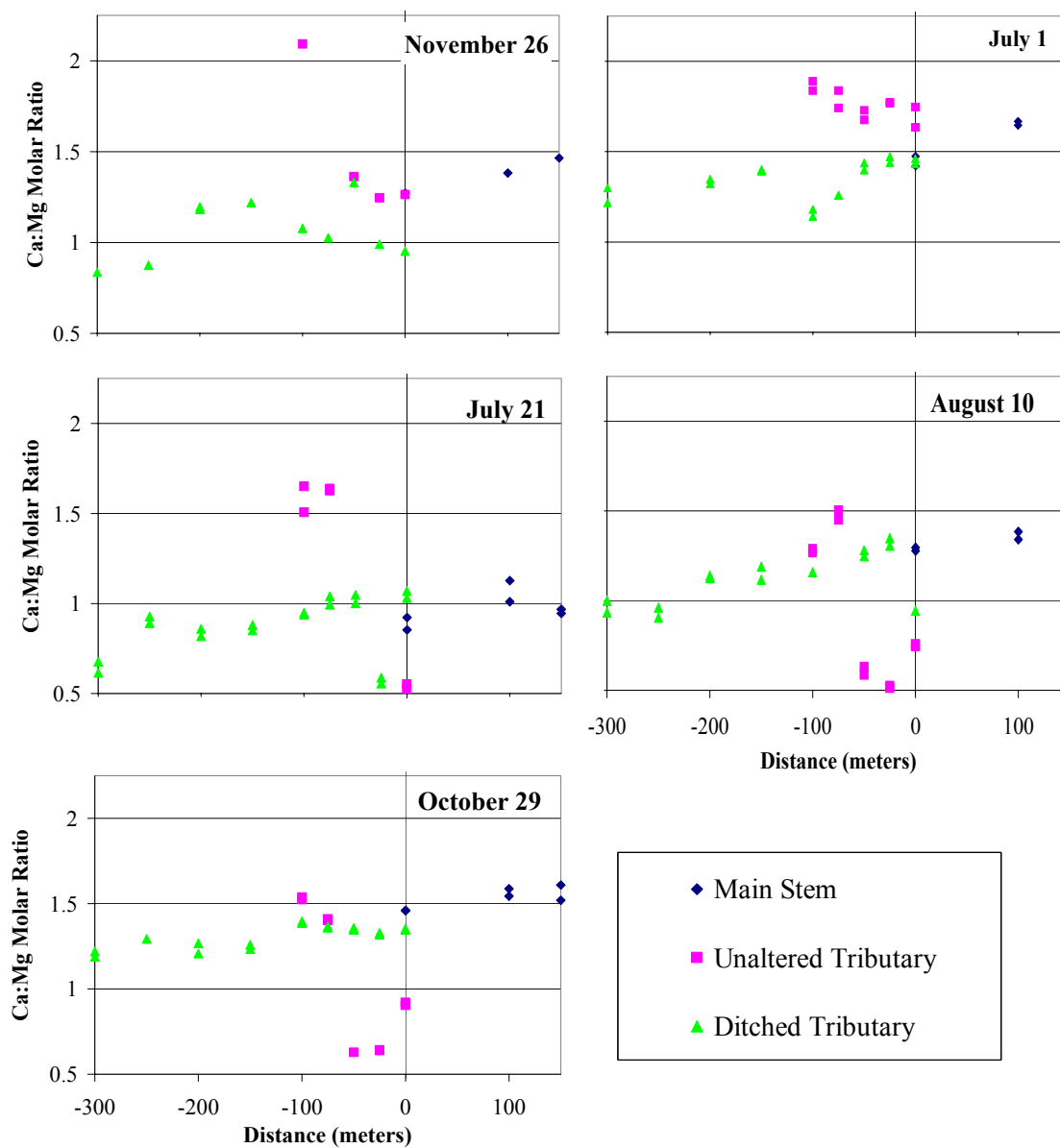
Figure 18. Spatial variation in the molar ratio between calcium and magnesium for each sample date. The molar ratio of dolomite is 1. Uncertainty is smaller than the symbol used.
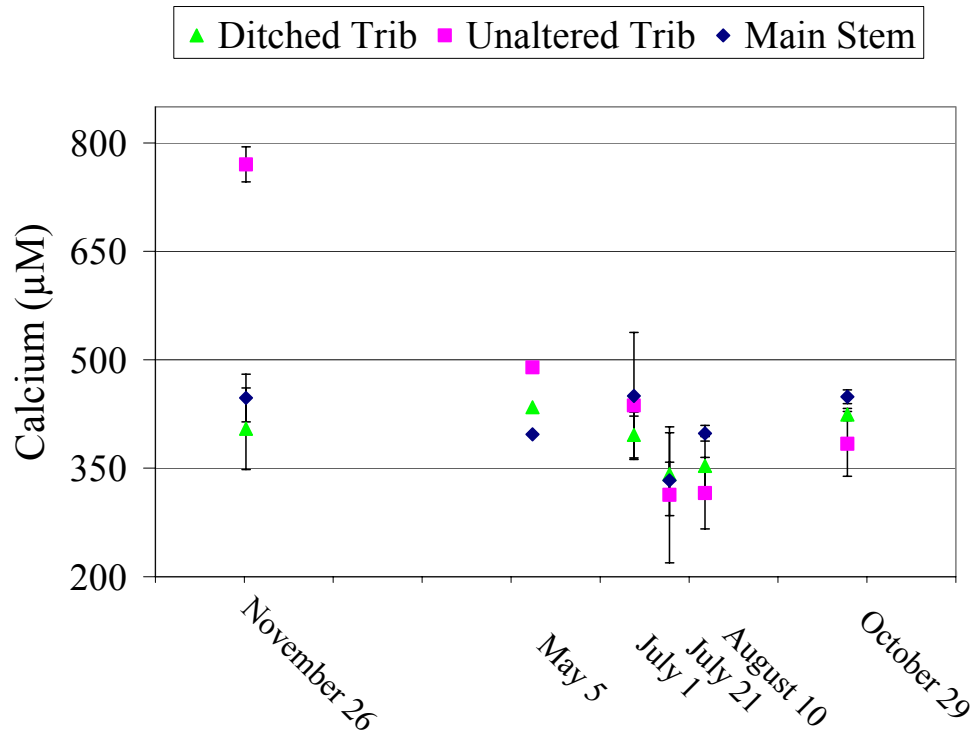
Figure 19.   Temporal variation in calcium. Each point represents the average of all value obtained along a given reach on a given sample date. Error bars show the standard deviation of values on a given sample date. On sample date May 5th measurements were only made on all three sections at the confluence and thus there is no data set to calculate standard deviation.
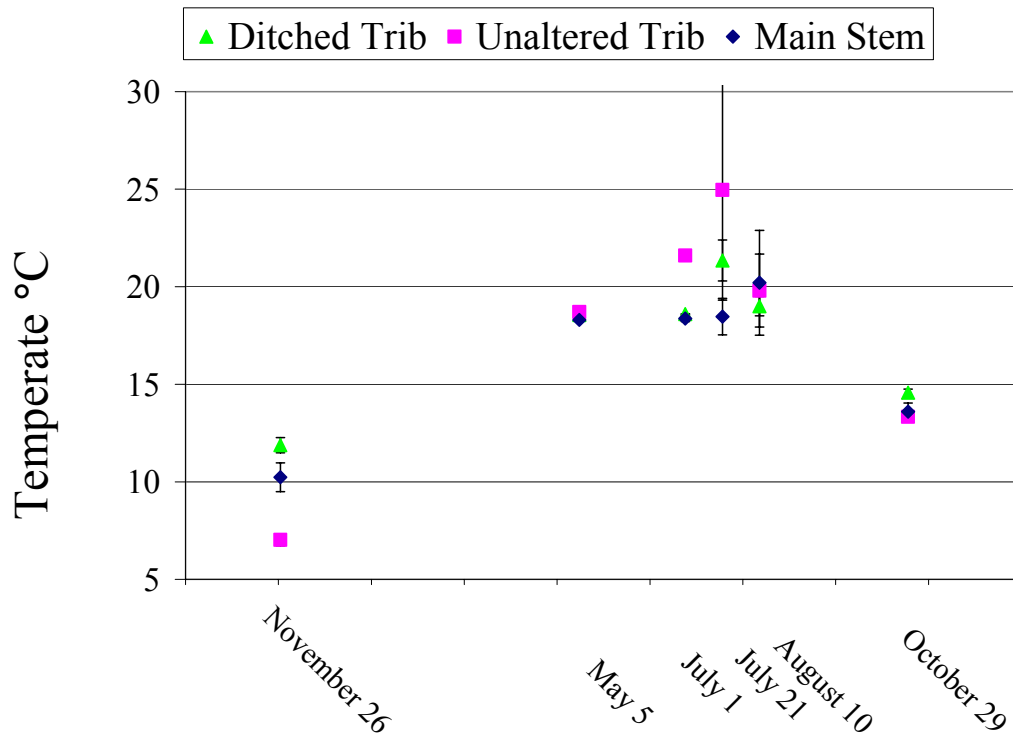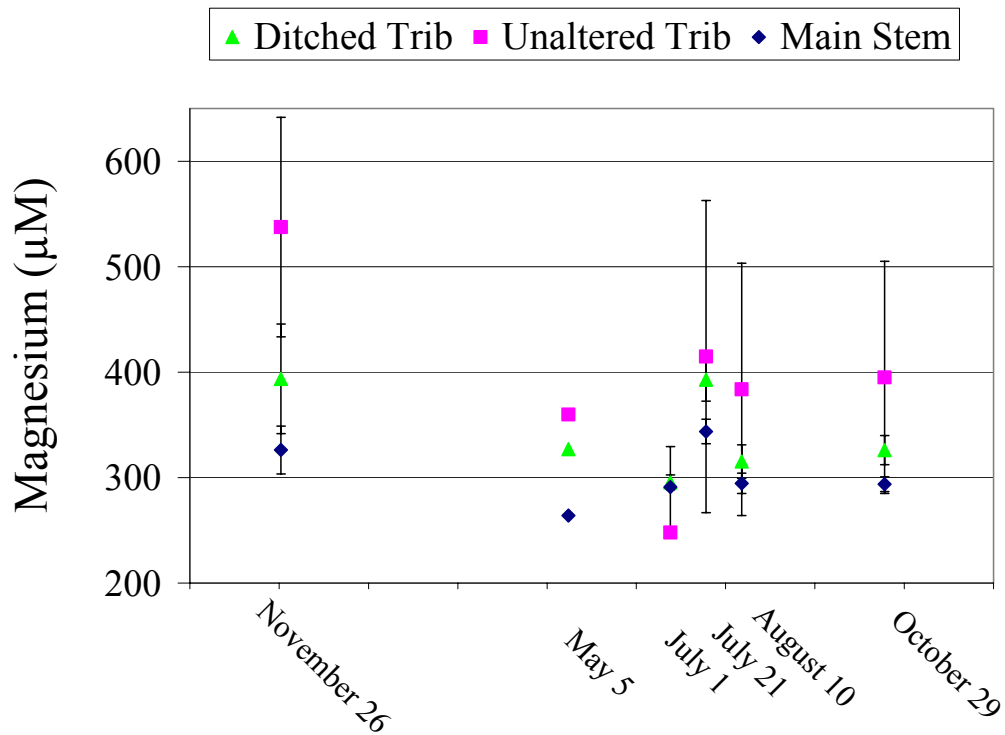
Figure 20. Temporal variation in magnesium. Each point represents the average of all value obtained along a given reach on a given sample date. Error bars show the standard deviation of values on a given sample date. On sample date May 5th measurements were only made on all three sections at the confluence and thus there is no data set to calculate standard deviation.
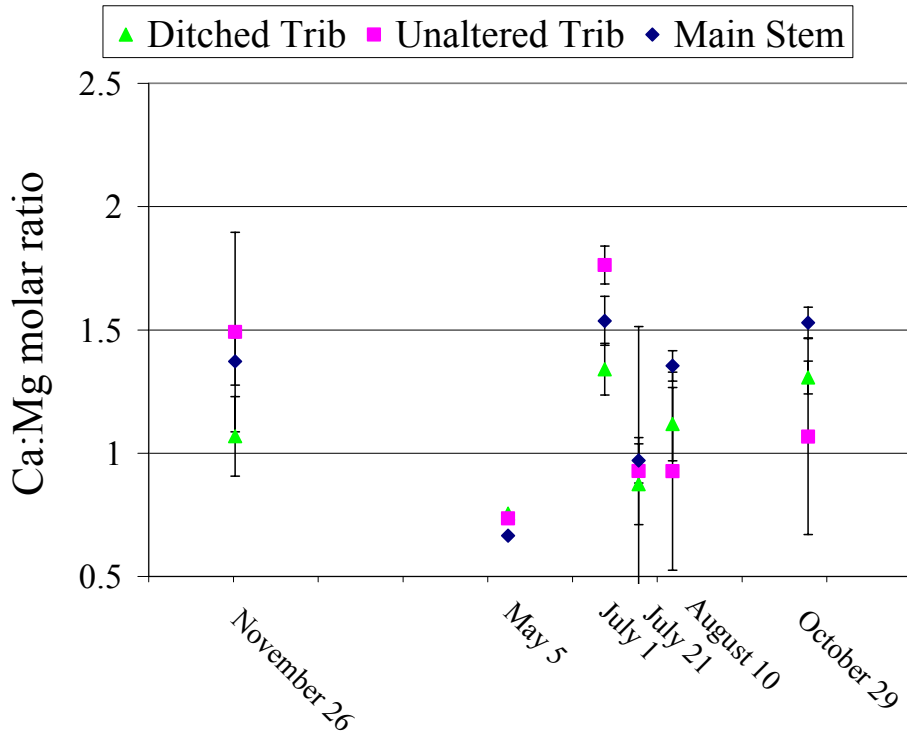
Figure 21. Temporal variation in calcium to magnesium ratio. Each point represents the average of all value obtained along a given reach on a given sample date. Error bar show the standard deviation of values on a given sample date. On sample date May 5th measurements were only made on all three sections at the confluence and thus there is no data set to calculate standard deviation.

3.2.3 Sodium

The average sodium concentration across all sites is 0.13 (± 0.86) μmolar. Leaving out six anomalously high values from sample date 11-26-03 yields a 0.11(± 0.03) μmolar average. Charge balance calculations, averaged over all sites, show that sodium accounts for only 0.007% of total positive charge.

3.2.4 Nitrate

Nitrate measurements are shown graphically for each sample date in Figure 22. Nitrate concentrations in the unaltered tributary increase along the reach on each sample date. With the exception of July 1st, nitrate concentrations in the ditched

tributary decrease on each sampling date. Nitrate concentrations at sample sites NT-100 and NT-75 are consistently the lowest values of all sites on a given sample date. Nitrate concentrations on July 21st, August 10th, and October 29th were at or below detection limit. On these dates, the remaining unaltered tributary sites are close to ditched tributary values of comparable distance from the confluence. On November 26th and July 1st unaltered tributary nitrate concentrations are consistently lower than any ditched tributary value. Whole site averaged temporal variations are shown in Figure 23. The unaltered tributary consistently has the lowest nitrate concentrations, while the ditched tributary consistently has the highest. The main stem nitrate concentrations are closer to ditched tributary values, again indicating a relatively higher contribution than the unaltered tributary.
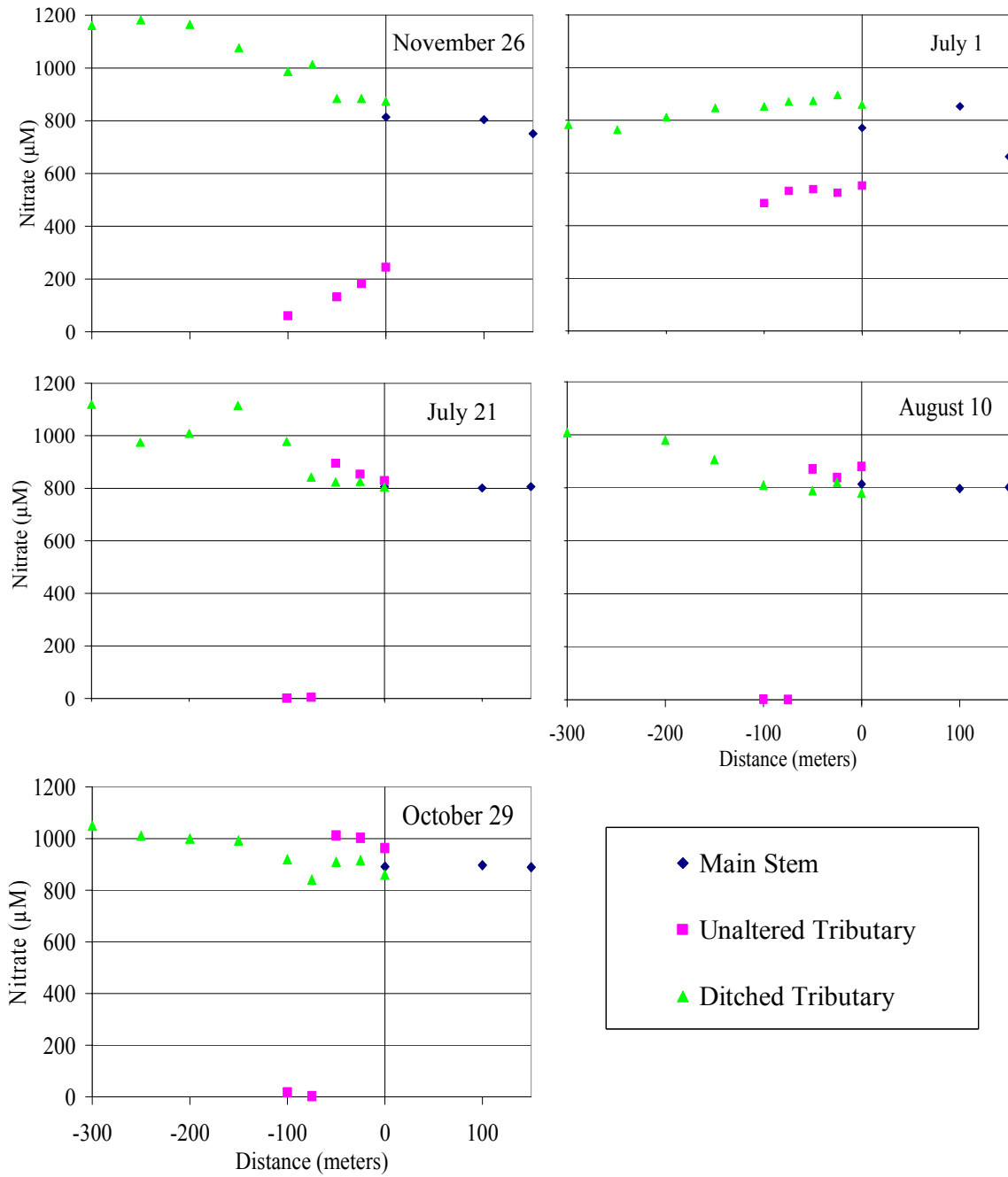
Figure 22. Spatial variation in nitrate concentration for each sample date. Uncertainty in these measurements is smaller than the symbol size used.
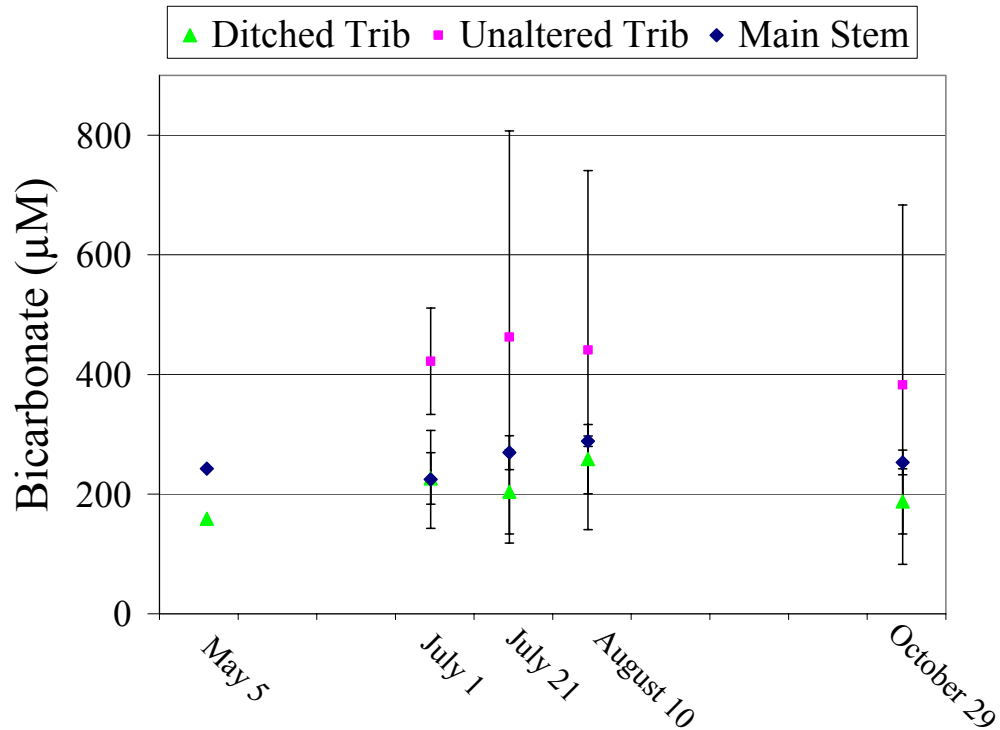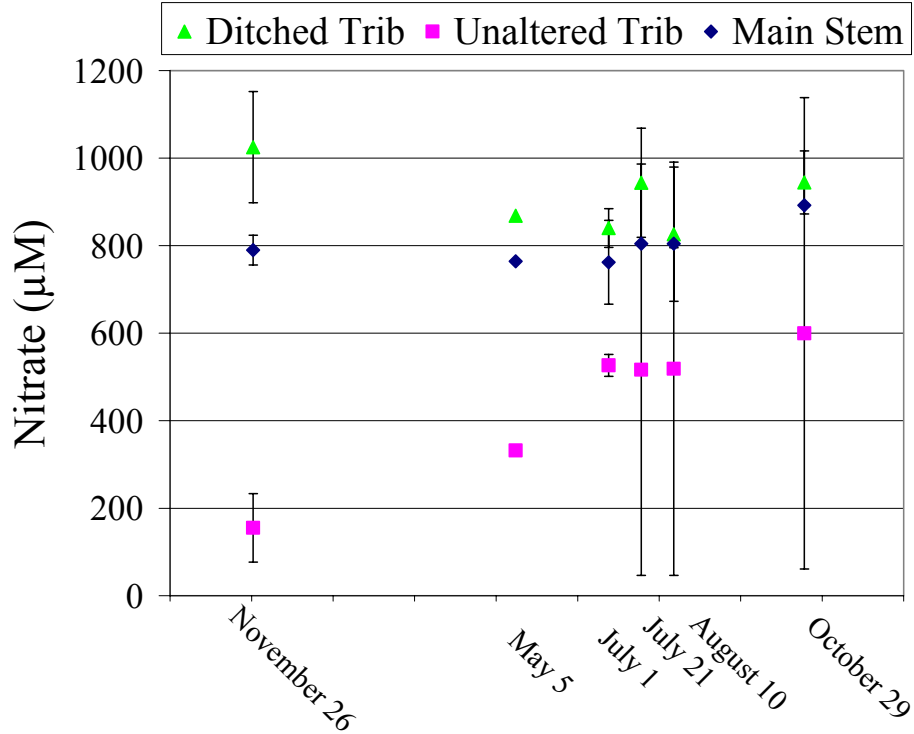
Figure 23. Temporal variation in nitrate. Each point represents the average of all value obtained along a given reach on a given sample date. Error bars show the standard deviation of values on a given sample date. On sample date May 5th measurements were only made on all three sections at the confluence and thus there is no data set to calculate standard deviation.

3.2.5 Dissolved Inorganic Carbon Isotopes

Figure 24 shows the carbon isotopic data for dissolved inorganic carbon (DIC) on each sampling date. The DIC isotopic signature experiences greater fluctuation and less clear trends than many of the other chemical parameters. Notably, on the two winter sampling dates there was no algae or other plant material growing in the stream channel (November 26th and October 29th) and on these dates the unaltered tributary shows a clear trend to more ^{13}C depletion downstream while the ditched tributary shows a trend to more ^{13}C enrichment downstream.

52

On the other hand, trends on the other three summer sampling dates are not as clear. On sample dates July 1st, July 21st, and August 10th the ditched tributary appears to oscillate around a value of -10 ‰. The unaltered tributary trends are more difficult to decipher as a result of the relatively shorter extent of the stream. July 1st shows no appreciable trend. July 21st shows heavy values in the upper reaches and relatively light values in the lower reach. August 10th shows no appreciable trend.

Whole stream average temporal variations are shown in Figure 25. The greatest variation is on November 26th and the least on July 21st. Sample date August 10th is marked by substantially heavier values. The two winter sample dates are relatively lighter.
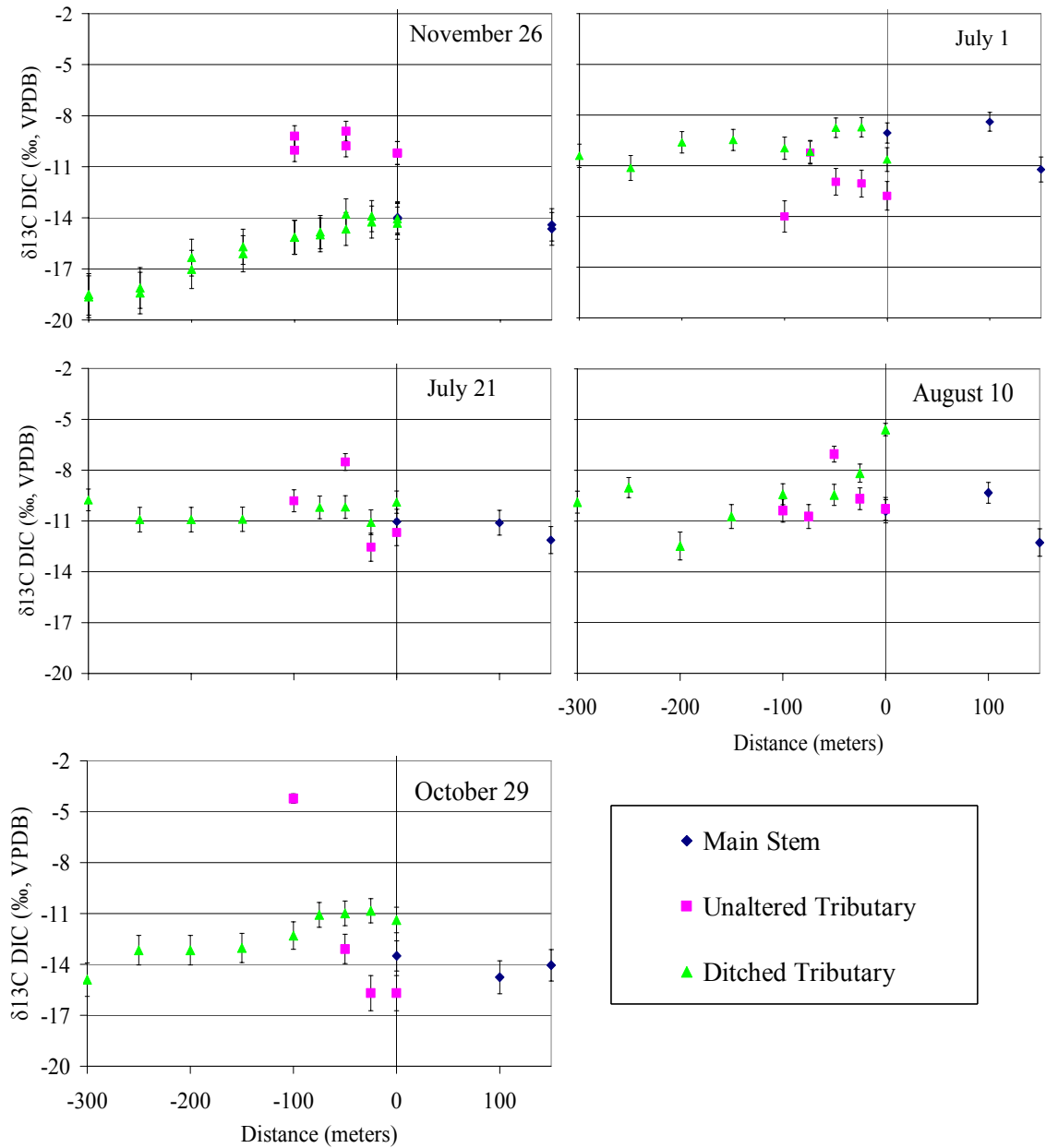
Figure 24. Spatial variation in DIC carbon isotopes for each sample date. Values are reported relative to Viennea PeeDee Belemnite (VPDB) standard, a Cretaceous-aged mollusk.
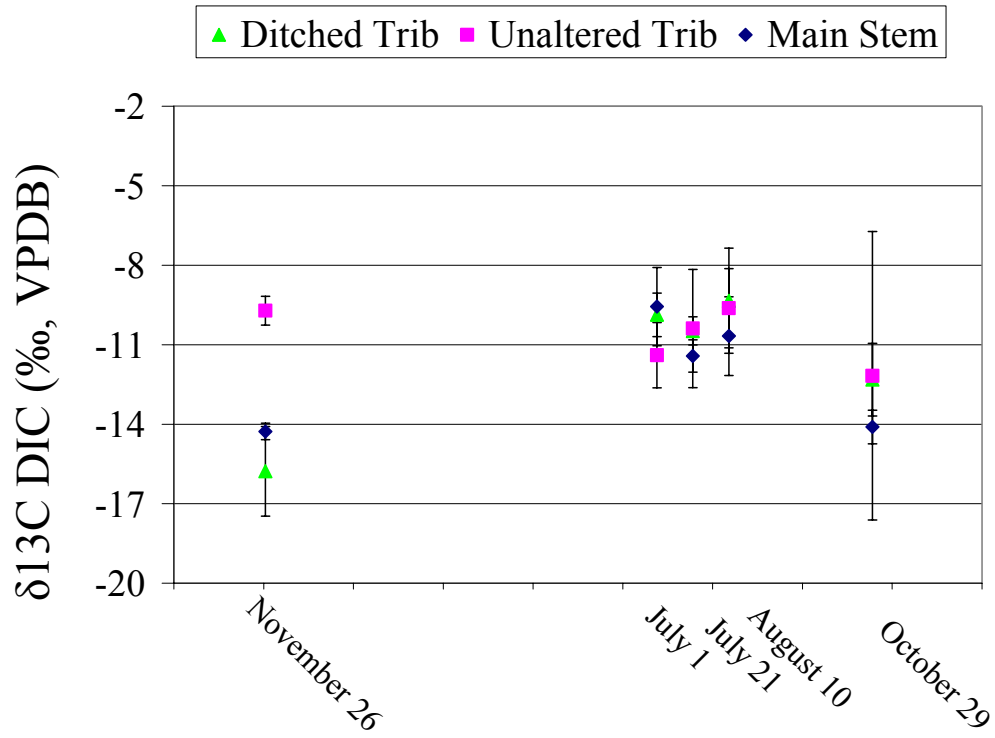
Figure 25.   Temporal variation in carbon isotopic values. Each point represents the average of all value obtained along a given reach on a given sample date. Error bars show the standard deviation of values on a given sample date.

3.2.6 Algae Isotopes

Table 3 shows the algae isotopic values and C:N ratios of all measured algae samples including the one-sigma uncertainty for each value. No appreciable pattern is present in the $^{13}$C data. The average value of ^{13}C in plant algae is -36.6 with a 1σ uncertainty of ± 2.6 ‰. Notably the proportion of ^{15}N in the algae from the uppermost unaltered tributary is substantially higher than other measured samples. Excluding these samples the average is 4.2 ‰ with a 1σ uncertainty of ± 1.0 ‰. Values of 8.8 ‰ and 12.4 ‰ are well outside this uncertainty.

Table 3. Algae nitrogen and carbon isotopic values.

Date	Sample	Distance	δ^{13}C (‰, VPDB)	error	δ^{15}N (‰, air)	error
10/29/2004	DT-300	-300	-32.51	0.03	4.06	0.05
10/29/2004	DT-300	-300	-32.37	0.12	4.31	0.09
10/29/2004	DT-250	-250	-39.34	0.08	4.21	0.04
10/29/2004	DT-150	-150	-33.77	0.03	3.91	0.05
10/29/2004	DT-100	-100	-37.11	0.03	4.34	0.05
10/29/2004	DT-75	-75	-35.94	0.03	5.52	0.05
10/29/2004	DT-60	-60	-37.63	0.08	4.00	0.04
10/29/2004	NT-50	-50	-36.55	0.03	4.06	0.05
10/29/2004	NT-100	-100	-35.84	0.16	12.35	0.09
10/29/2004	NT-85	-85	-35.26	0.16	8.80	0.09
7/21/2004	MS-0	0.1	-37.94	0.12	4.20	0.09
7/21/2004	NT-55	-55	-36.17	0.16	2.14	0.09
7/21/2004	NT-0	-0.1	-40.02	0.03	4.33	0.05
7/21/2004	DT-0	-0.1	-40.40	0.16	3.76	0.09
7/21/2004	DT-250	-250	-40.11	0.03	3.14	0.05
7/21/2004	DT-300	-300	-34.87	0.08	6.66	0.04

3.2.7 Flow Data

Problems were encountered in directly measuring the flow of water through these tributaries. The traditional method uses a flow meter to determine incremental depths and velocities. Integrated over the entire channel, discharge can be calculated.

The streams involved in this study were relatively small and on the lower end of feasibility for this method. A combination of additional factors prevented accurate measurements. Those factors included 1) water too shallow for the propeller, 2) semi-solid bottom, 3) inundation with plant material, and 4) extremely slow velocities.

Discharge measurements would provide three pieces of useful information. First, accurate measurements might show an increase in volume along each of the stream reaches that would enable quantification of discharging groundwater from headwaters to confluence. Unfortunately, there is not a direct alternate source of such information. Visible upwelling springs along each of the reaches as well as the previous work of Bohlke and Denver (1995) and Bachman et al. (2002) suggest that there is, in fact, a significant contribution from groundwater. The chemical characterization of the regional aquifers enables the use of chemical changes as a proxy for volumetric changes.

Second, discharge measurements would provide a quantification of the relative contributions of the natural and ditched tributaries to the main stem. In the absence of flow data, three chemical parameters have been selected (temperature, alkalinity, and nitrate concentration) to use in a simple mixing equation to quantify the relative contribution of each to the main stem. A measurement of each of these values was taken in each tributary directly above the confluence, as well as directly below the confluence. The simple mixing equation assumed instantaneous mixing and no groundwater contribution.

$$MS = (DT * X) + (DT * (1-X)) \tag{7}$$

$$X = (MS – UT) / (DT - UT) \tag{8}$$

Where: MS = concentration in the main stem

DT = concentration in the ditched tributary

UT = concentration in the unaltered tributary

Table 4 shows the relative contributions of each, and the standard deviation of the estimate. Clearly there are some problems with the assumptions, and this shows in the high standard deviation. Even with these uncertainties it is nonetheless clear that the ditched tributary accounts for a greater percentage of flow.

Table 4.   Proportional contribution of unaltered tributary and ditched tributary based on nitrate, alkalinity, and temperature measurements.

Sample Date	Unaltered Tributary	Ditched Tributary	Standard Deviation
11/26/03	0.08	0.92	± 0.03
7/1/04	0.13	0.87	± 0.16
7/21/04	0.08	0.92	± 0.10
8/10/04	0.14	0.86	± 0.35
10/29/04	0.11	0.89	± 0.19

Thirdly, flow measurements would enable comparison of high and low base flow conditions. Morgan Creek, the adjacent and slightly larger watershed, is equipped with a USGS gauging station. The discharging groundwater in the two watersheds comes from the same aquifer, so this stream would likely represent a good proxy for the study site. Rain storm events would likely affect the watersheds in a similar way based on spatial relationships. Figure 26 shows the mean stream flow for ten days preceding and ten days following each sample event. The date of sampling is marked with a star.
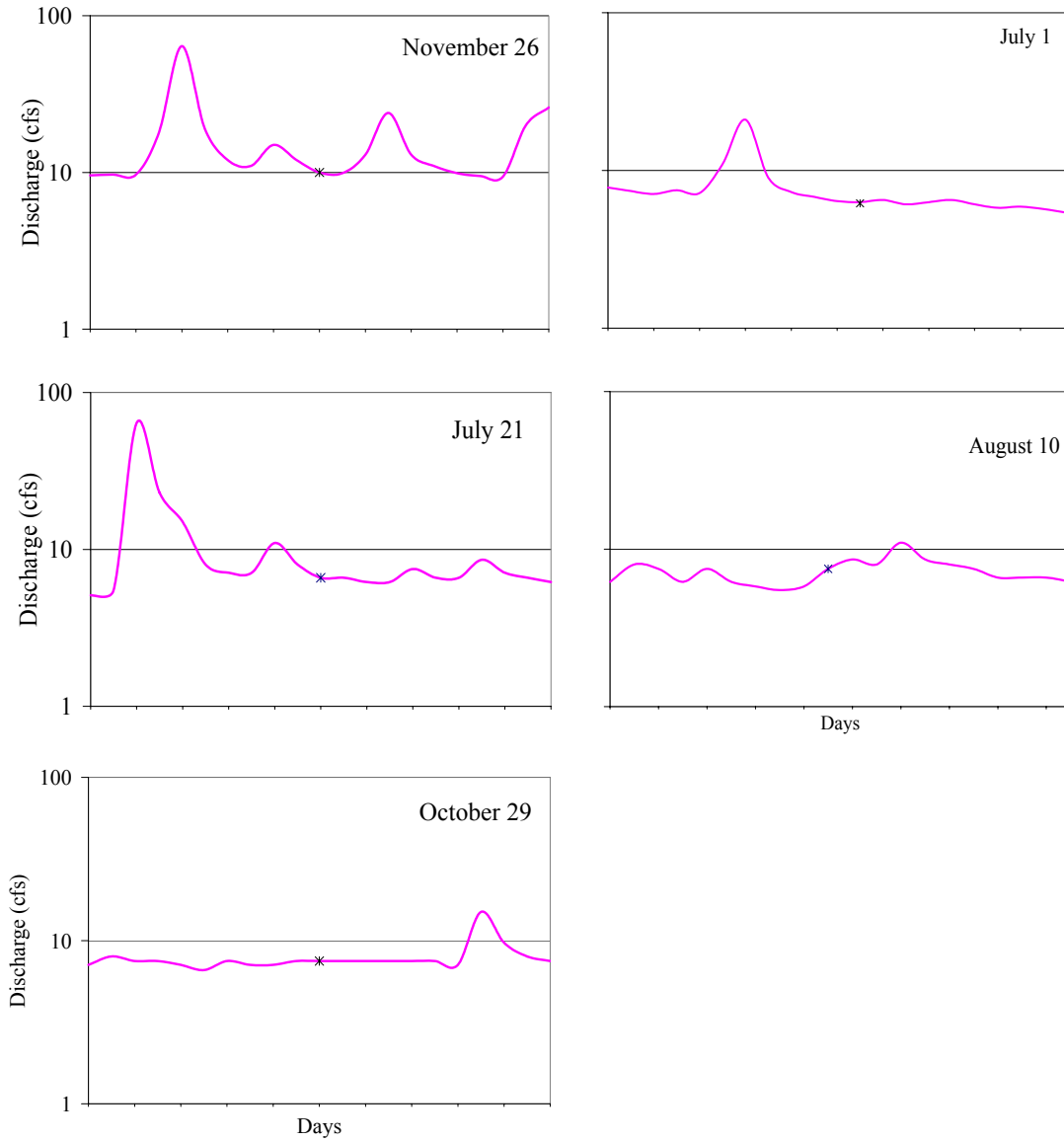
Figure 26. Daily mean discharge values for ten days prior to and after each sample date of Morgan Creek, adjacent watershed of Chesterville Branch. Values obtained through use of USGS real-time feature at water.usgs.gov.

Chapter 4: Discussion

4.1 Flow Conditions

Samples were taken under base flow conditions. The criteria necessary for a

sampling to occur was zero precipitation for two days prior based on the local

Chestertown, Maryland rain gauge. Base flow conditions exist when there is no

precipitation event water in the stream. Return to a base flow after a precipitation can

be gauged on a hydrograph by determining when the stream returns to a pre-storm

steady state level. Without replenishment, base flow would eventually decline to zero

(Fetter, 1994). Analysis of the adjacent Morgan Creek allows an approximate

estimate of relative base flow conditions. Table 5 shows the average stream

discharge for each sample date in Morgan Creek.

Table 5.
Mean discharge from
adjacent Morgan Creek
on each sampling date.

Sample Date	Average (cfs)
November 26th	10
July 1st	6.3
July 21st	7.3
August 10th	8.3
October 29th	7.5

These values suggest a relatively higher base flow in the winter months, and

lower base flow in the summer months. Figures 26 shows where these discharge

values fit into flow conditions directly preceding and following the sample dates.

Sample dates July 1st and October 29th each follow several days of steady base flow.

Sample dates November 26th and July 21st appear to fall on base level, however

between storm events on either side. On the actual sample date, stream level appears

to have returned to base flow. Sample date August 10th appears to fall along a slight

increase in base level condition.

4.2 Chemical Composition

4.2.1 Charge Balance

The chemical composition of surface water samples holds valuable

information that enables the reconstruction of the geologic, hydrologic, and biologic

history of a parcel of water. Water is necessarily electrically neutral, meaning every

cation that enters solution through mineral dissolution or other physical or biologic

reaction must be accompanied by an anion. The measured constituents include $[OH^-]$,

$[H^+]$, $[HCO_3^-]$, $[Ca^{2+}]$, $[Mg^{2+}]$, $[NO_3^-]$, and $[Na^+]$. According to Stumm and Morgan

(1996) and Bohlke and Denver (1995), $[Cl^-]$, $[K^+]$, and $[SO_4^{2-}]$ are also likely as major

ions. Charge balance calculations in this study were made by inferring concentration

of sulfate, chloride, and potassium from Bohlke and Denver (1995) and Stumm and

Morgan (2002).   The charge balance calculations show a slight excess in negative

charge which is one to two orders of magnitude smaller than calcium, magnesium,

nitrate, bicarbonate, and chlorine concentrations. This excess is greater than the

combined concentrations of sulfate, sodium, and potassium. The average major ion

concentrations of the Aquia aquifer is shown in Table 6. These values are averaged

from groundwater samples taken by Bohlke and Denver (1995), Bachman and others

(2002), and Ator and others (2005). Notably the calcium to magnesium molar ratio

yields a much higher proportion of calcium than would be expected based solely on

dolomite dissolution. This suggests that spatially in the surficial aquifer there are

additional sources of calcium other than anthropogenic dolomite dissolution.

Bicarbonate is roughly 100 µM less than simply adding the molar concentrations of

calcium to magnesium, which suggests either a sink of subsurface bicarbonate or a

source additional to dolomite and carbonate dissolution. The likely source is the

chemical and physical weathering of silicates in the subsurface. Nitrate concentration

is three and a half times the maximum contaminant level suggested by the

Environmental Protection Agency. Carbon-13 abundance is slightly more enriched

that that expected solely by soil gas exchange (-21‰).

Table 6. Average major ion concentrations of the Aquia aquifer
(Bohlke and Denver, 1995; Bachman et al., 2002).

Temp ($^\circ$C)	16.1
pH	5.81
Ca^{2+} (µM)	410
Mg^{2+} (µM)	165
Ca:Mg	2.5
Na^+ (µM)	175
K^+ (µM)	79
HCO_3^- (M)	365
^{13}C (‰)	-15.5
Cl^- (µM)	165
NO_3^- (µM)	556

4.2.2 pH

pH is a measure of hydrogen ion concentration. At any given time, the sum of

pH and pOH must be equal to 14.

$$pH = -\log [H^+] \tag{9}$$

$$pOH = -\log [OH^-] \tag{10}$$

$$pH + pOH = 14 \tag{11}$$

$$[H^+] * [OH^-] = 10^{-14} \tag{12}$$

Changes in pH can be indicative of a variety of chemical reactions. Some reactions, such as denitrification, produce [H^+], while others, such as the dissolution of limestone consume [H^+] (Bohlke, 2002). The effect such reactions have on measurable pH is limited due to the buffering capacity of natural waters. Dissolved inorganic carbon absorbs either [H^+] or [OH^-] minimizing the impact. Buffering is discussed in further detail in the following section.

The average pH value of the Aquia aquifer is 5.8 (Bohlke and Denver, 1995; Bachman et al., 2002). In this study, the pH trend is decreasing along the unaltered tributary and increasing along the ditched tributary. The discharge in the ditched tributary headwaters is relatively acidic and increases in pH towards the confluence. Sample date November 26th exhibits the steepest increase (1.9 pH units/ km, equations found in Appendix C). Measurements on this date are most indicative of pure groundwater-surface water interactions in the absence of plants and algae. Bohlke and Denver (1995) observed a hydrogen ion concentration gradient in the Aquia aquifer. The increasing pH along the ditched tributary is most-likely a result of dilution by deeper, more basic Aquia groundwater.

4.3 Major Ion Constituents

4.3.1 Alkalinity

The many chemical changes resulting from faunal uptake, physical reactions, reduction/oxidation reactions, and bacterially-mediated reactions all change the chemical and isotopic composition of a system. Many of these reactions result in either the release or consumption of H^+ ions. A buffer is defined as a mixture of an

acid and its conjugate base that has the ability to absorb either OH^- or H^+ ions. Rivers are buffered by dissolved inorganic carbon (DIC) derived from exchange with atmospheric CO_2 and the dissolution of carbonates and silicate through weathering reactions.

The buffering of natural systems results from the dissolution of atmospheric carbon dioxide. Carbon dioxide dissolves in water according to the formal reaction:

$$CO_2\ (aq) + H_2O \rightarrow H_2CO_3 \tag{13}$$
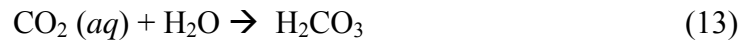
Because the two forms are chemically equivalent the standard is to refer to the sum of the concentrations of both species as $H_2CO_3{}^*$ (Stumm and Morgan, 1996)

$$CO_2 + H_2CO_3 = H_2CO_3{}^* \tag{14}$$

This compound is a diprotic acid, that is, has the ability to give up two hydrogen ions detailed in the reactions below.

$$H_2CO_3{}^* \leftrightarrow H^+ + HCO_3{}^- \qquad\qquad K_{a1} = 10^{-6.3} \tag{15}$$

$$HCO_3{}^- \leftrightarrow H^+ + CO_3{}^{2-} \qquad\qquad K_{a2} = 10^{-10.3} \tag{16}$$

The total concentration (C_T) of DIC is the sum of the concentrations of the carbonate species present.

$$C_T = [H_2CO_3{}^*] + [HCO_3{}^-] + [CO_3{}^{2-}] \tag{17}$$

In a closed system, C_T is a constant value. The proportion of each species is a function of pH as shown in Figure 27.
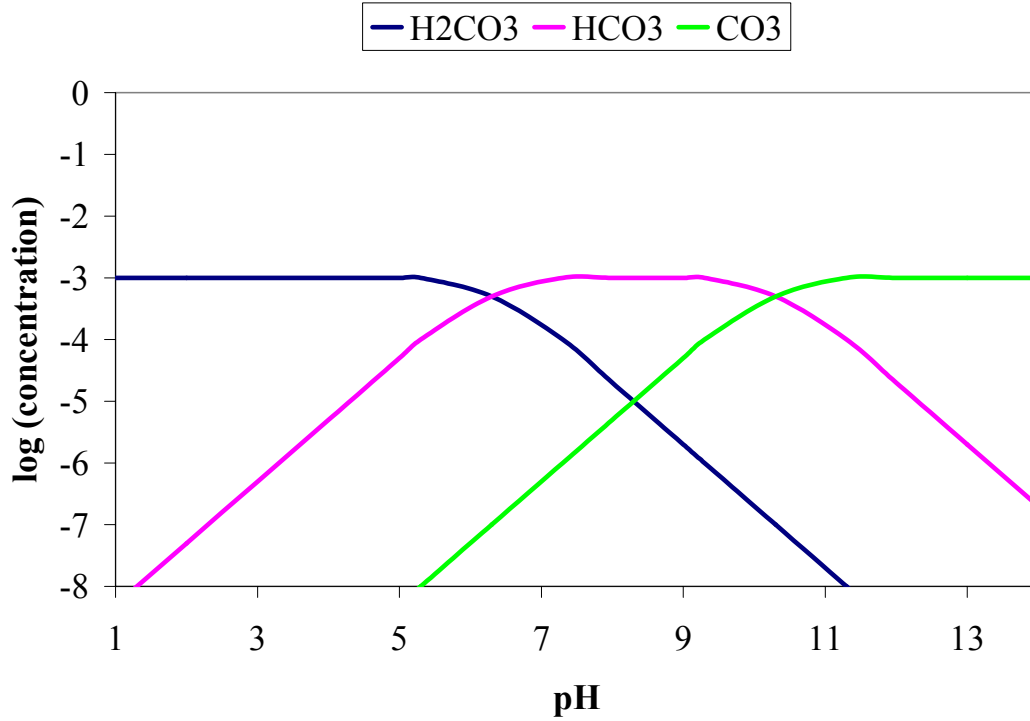
Figure 27. Dissolved inorganic carbon speciation in an open system at a total concentration of 10^{-3} molar.

In an open system, C_T is variable. The concentration of H_2CO_3* is a function of the CO_2 solubility and the atmospheric partial pressure of CO_2. Mathematically this is given as:

$$\left[H_2CO_3{}^*\right] = \left[\left(P_{CO_2}\right)\left(K_H\right)\right]$$ (18)

Where P_{CO_2} = atmospheric partial pressure of CO_2 = $10^{-3.5}$

K_H = Henry's constant = $10^{-1.5}$

The concentrations of the other species are dependent upon the concentration of $H_2CO_3{}^*$ and pH. The acidity constants (K_a) define speciation between $H_2CO_3{}^*/HCO_3^-$ and HCO_3^-/CO_3^{2-}.

$$K_{a1} = \frac{\left[HCO_3^-\right]\left[H^+\right]}{\left[H_2CO_3{}^*\right]} = 10^{-6.3}$$ (19)

$$K_{a2} = \frac{\left[CO_3^{2-}\right]\left[H^+\right]}{\left[HCO_3^-\right]} = 10^{-10.3} \tag{20}$$

As shown in Figure 27, pK_{a1} and pK_{a2} correspond to the pH values in a closed system where there are equal parts H_2CO_3 / HCO_3^- and HCO_3^- / CO_3^{2-} respectively. The K_a equations can be rearranged to define HCO_3^- and CO_3^{2-} concentrations in terms of $[H^+]$, acidity constants, K_H, and P_{CO_2}.

$$\left[HCO_3^-\right] = \frac{K_{a1}\left[H_2CO_3\right]}{\left[H^+\right]} = \frac{K_{a1}\left[(K_H)(P_{CO_2})\right]}{\left[H^+\right]} \tag{21}$$

$$\left[CO_3^{2-}\right] = \frac{K_{a2}\left[HCO_3^-\right]}{\left[H^+\right]} = \frac{K_{a2}K_{a1}\left[(K_H)(P_{CO_2})\right]}{\left[H^+\right]^2} \tag{22}$$

Thus the total concentration of DIC (C_T) can be written as a function with a single variable, $[H^+]$.

$$C_T = \left[(P_{CO_2})(K_H)\right] + \frac{K_{a1}\left[(K_H)(P_{CO_2})\right]}{\left[H^+\right]} + \frac{K_{a2}K_{a1}\left[(K_H)(P_{CO_2})\right]}{\left[H^+\right]^2} \tag{23}$$

Figure 28 shows the speciation of DIC in an open system. The concentration of $H_2CO_3^*$ is constant and not dependent on pH. The concentration of HCO_3^- increases with a slope of 1 with each pH unit, and the concentration of CO_3^{2-} increases with a slope of 2 with each pH unit. Measured pH values in this study range from 4.9-7.0. At these values, the concentration of carbonic acid is roughly three orders of magnitude lower than the other two species. Therefore it can be ignored, which allows simplification of the above equation to:

$$C_T = \left[(P_{CO_2})(K_H)\right] + \frac{K_{a1}\left[(K_H)(P_{CO_2})\right]}{\left[H^+\right]} \tag{24}$$
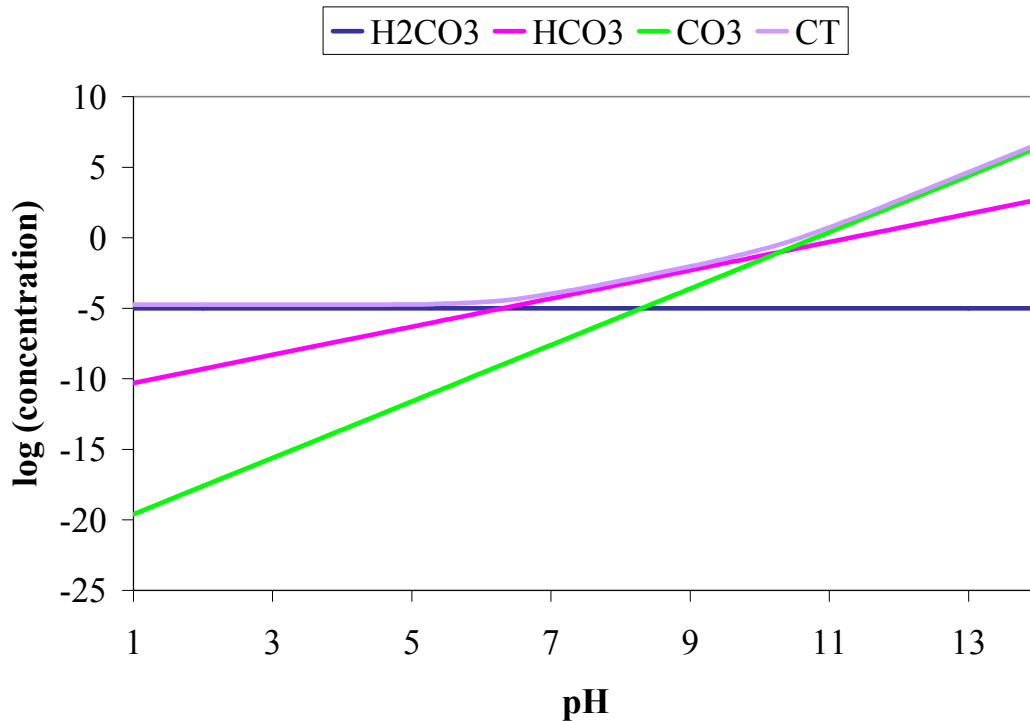
Figure 28. Dissolved inorganic carbon speciation in an open system.

The digital titration failed to measure any phenolphthalein alkalinity. Calculations based on pH confirm the concentrations of each hydroxide and carbonate are at least two orders of magnitude lower than bicarbonate. According to the HACH method the alkalinity of all measured samples is equal to the bicarbonate concentration.

Bohlke and Denver (1995) measured DIC concentrations 30-50 times greater than would be expected of water equilibrated with open air. They interpreted this excess as organically-produced soil CO_2. Calculations were made to predict the expected bicarbonate concentrations based solely on the partial pressure of CO_2 in the atmosphere and pH. Actual bicarbonate concentrations were one to two orders of magnitude greater than calculated values suggesting other sources of alkalinity,

namely the dissolution of limestone or dolomite and silicate weathering. Both possible mechanisms for nitrate removal, photosynthesis and denitrification, result in an increase in alkalinity. Alkalinity concentrations at sites NT-100 and NT-75 are substantially elevated on all sample dates except July 1st. This supports the theory of denitrification in the stagnant reach followed by dilution of lower DIC groundwater. Bicarbonate increased along the ditched tributary for all sample dates except July 1st. The increase is slight but suggests addition of bicarbonate. Bohlke and Denver (1995) did not report a vertical gradient in bicarbonate, however the results suggest either a systematic increase with alkalinity and depth or some other surficial source. Sample date July 1st does not follow the trends of the other sampling dates. This date notably coincides with a substantial increase in plant material and lower base flow.

4.3.2 Calcium

As indicated in Table 6 the average calcium concentration for the surficial Aquia aquifer is 409 μmolar. The higher calcium concentration in the Hornerstown aquifer is attributed to dissolution of the limestone-rich marine unit. The surficial aquifer gains calcium predominantly from dissolution of crushed dolomite used in agricultural fields to adjust the pH (Bohlke, 2000). Dolomite is loosely defined as having a 1:1 molar ratio of calcium to magnesium, while pure limestone is considered to have less than five weight percent magnesium (Boggs, 1995).

Calcium concentrations consistently increase along the ditched tributary and consistently decrease along the unaltered tributary. This is consistent with addition of more calcium-rich groundwater along the ditched tributary. The slight increase along the unaltered tributary is consistent with gaining relatively shallow groundwater with

similar chemical character along its reach. Calcium results are consistent with the proposed model.

4.3.3 Magnesium

Dissolved magnesium results from similar dissolution reactions as calcium, namely dissolution of either dolomite or limestone or silicate weathering. Surficial aquifer average concentrations are shown in Table 6. In the Aquia aquifer, magnesium results from the dissolution of dolomite which yields a 1:1 molar ratio of calcium to magnesium and a 1:1 molar ratio of carbonate to calcium plus magnesium.

Magnesium concentrations decrease along the ditched tributary on all sample dates except July 1st. This is consistent with addition of a deeper more dilute groundwater source along the reach.

Magnesium concentrations in the unaltered tributary do not fit the proposed model. This would predict that magnesium concentrations would remain relatively constant along the unaltered stretch. Discharging groundwater is expected to be of similar age, which should result in minimal variance along the stretch. This, however, is not the case. On all but the July 1st sample date, sample sites NT-50 and NT-25 are roughly double any other magnesium concentration measured in the unaltered tributary. The anomalous magnesium signature could be either a result of relatively high magnesium concentrations in sample sites NT-50 and NT-25 or relatively low magnesium concentration in sample sites NT-100 and NT-75. However, when plotted as magnesium versus calcium (Figure 29) it is clear that the high magnesium values are the anomaly and not the relatively lower values of NT-100 and NT-75. Figure 29 is modified from a figure originally published by Bohlke

and Denver (1995) to include data from this study. The lines on the graph represent various molar ratios of the two cations. The majority of the data from this study along with Bohlke and Denver values for the surficial aquifer plot along the 1:1 molar ratio. This is consistent with a crushed dolomite source for both the calcium and magnesium. The 2:1 molar ratio line is consistent with dilution by deeper groundwater with relatively lower magnesium concentrations. The 1:2 molar ratio line however does not have a physical explanation. There is no corresponding anomaly with the calcium data. This suggests that the anomaly results from an additional magnesium source rather than a phenomenon that preferentially removes calcium. The magnesium values at sites NT-100 and NT-75 are consistent with the proposed model. Theoretically sites NT-50 and NT-25 are fed by a similar groundwater source. At present, it is not clear what is producing the discrepancy.
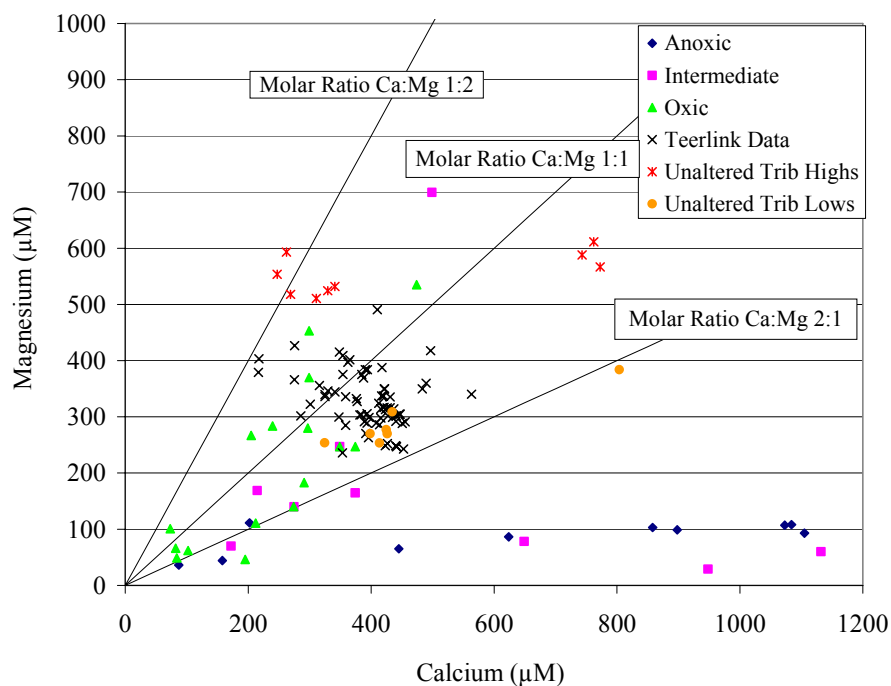
Figure 29.   Calcium versus magnesium concentration for samples within Locust Grove study site. Anoxic, intermediate, and oxic are defined by Bohlke and Denver (1995) as greater than 5 mg/L, between 2 mg/L and 5 mg/L, and less than 2 mg/L of dissolved oxygen, respectively.

Calcium and magnesium chemically behave in a similar manner. One factor that could affect these cation concentrations is the precipitation of certain minerals. Using the equilibrium constant for the solubility product (K_{sp}), cation concentration, pH, and alkalinity, calculations can be made to determine if it is thermodynamically possible for minerals, in particular calcite or magnesite, to precipitate.

$$K_{sp} = \left(Ca^{2+}\right)\left(CO_3^{2-}\right) \tag{25}$$

$$K_{sp} = \left(Mg^{2+}\right)\left(CO_3^{2-}\right) \tag{26}$$

$$K_{a2} = \frac{\left[CO_3^{2-}\right]\left[H^+\right]}{\left[HCO_3^-\right]} \tag{27}$$

71

$$K_{sp} = \frac{(Ca^{2+})(K_{a2})(HCO_3^-)}{(H^+)} \quad (28)$$

$$K_{sp} = \frac{(Mg^{2+})(K_{a2})(HCO_3^-)}{(H^+)} \quad (29)$$

The highest solubility product obtained through these calculations is 2 orders of magnitude undersaturated with respect to calcite and 3 orders of magnitude undersaturated with respect to magnesite. The low concentrations of each suggest that a solid phase does not play a role in this system

Other potential contributors to the magnesium anomaly are cation exchange with the soil, manganese oxide coatings on pebbles at NT-50 and NT-25, or decay of plant material upstream. Theoretically calcium and magnesium would behave similarly in cation exchange reactions, but to ultimately establish this relationship batch sorption experiments must be conducted (Evans, 1989). Below sample site NT-75 the pebbles in the stream bed of the unaltered tributary are coated with manganese oxide. The increase in velocity below this section results in oxygenation of the water. The black coating of the pebbles suggests that water upstream of this section was reduced enough for manganese to become mobile; as oxygen is added to the water manganese oxides form this black veneer. Manganese-oxide coatings are notorious for sorptive properties, especially of large cations. Calcium is relatively larger than magnesium and thus may be preferentially removed. While this explanation would help with regard to interpreting the calcium to magnesium molar ratios, it is clear from the data that the anomaly lies with magnesium concentrations at this point. Some mechanism is acting to release magnesium. It may be related to the

oxygenation of the water through this stretch, or alternatively related to the decay of plant material upstream.

4.3.4 Calcium to Magnesium Ratio

Magnesium, like nitrate, is indicative of anthropogenic agricultural influence. Unlike nitrate, magnesium is not altered, but rather moves conservatively through the system. In order for a decreasing nitrate trend to indicate denitrification along either of the Chesterville tributaries it should be coupled with steady calcium to magnesium ratio. If the calcium to magnesium ratio is instead increasing as a function of distance towards the confluence, this indicates dilution by a deeper more dilute groundwater.

Bohlke and Denver (1995) found that deep old waters had variable calcium concentration, but low magnesium concentrations and shallow young waters had relatively higher magnesium concentrations (Figure 29). They interpreted this as the shallower oxic groundwater being in hydrologic communication with these tributaries. Dolomite used to adjust soil pH contributes magnesium to the system. All samples from this study plot along the 1:1 molar ratio line, which suggests that in the 1st-order tributaries all of the contributing water is from the shallow and oxic Aquia aquifer. This is congruent with an understanding of 1st-order tributaries, which suggests that discharging water is relatively young, and follows a shallow flow path. Thus any anoxia or denitrification must be due to surface processes.

The calcium to magnesium ratio increases along the ditched tributary at each sampling date. This is consistent with a decreasing anthropogenic influence, resulting from dilution by a deeper more dilute groundwater source.

The anomalously low magnesium values discussed previously results in anomalous calcium to magnesium ratios in the unaltered tributary. The details of this inconsistency are discussed fully in the magnesium section.

4.3.5 Nitrate

Nitrogen fixation refers to 'fixing' nitrogen to a bioavailable form. Gaseous nitrogen has a triple covalent bond resulting in a stable gas. Before the introduction of synthetic fertilizers, nitrogen fixation resulted from microbes on roots of some plants and lightning strikes. Anthropogenic nitrogen fixation has resulted in unmanageable loads of nitrate and thus the problem of eutrophication. In the warmer non-winter months, the streams are typically choked with macroalgae.

Nitrate concentrations increase along the unaltered tributary at all sample dates. The low nitrate concentrations in the uppermost sample sites in the unaltered tributary are thought to be caused by local denitrification due to the stagnancy of the water. The slow moving water allows for the consumption of all dissolved oxygen resulting in an anoxic site and denitrification. Further towards the confluence, groundwater discharges in the unaltered tributary delivering additional nitrate. This results in an increasing nitrate trend overall.

The ditched tributary shows a decreasing trend on all sample dates except July 1st. Decreasing nitrate concentrations along the ditched tributary are consistent with the theory of dilution by older and deeper Aquia groundwater. Other possible contributions to declining nitrate concentration are hyporheic denitrification or plant uptake of nitrate. The steepest decline coincides with the two winter sampling dates. Nitrate persists both above and below the water table. When the water table rises,

this may flush nitrate from the previously dry soil. Thus, at higher base flow

conditions, nitrate concentration decrease at a steeper rate due to flushing at the

uppermost reaches of the tributary.

4.3.6 Dissolved Inorganic Carbon Isotopes

There are two naturally occurring stable carbon isotopes; ^{13}C with an

abundance of 1.11% and ^{12}C with an abundance of 98.89% (Stumm and Morgan,

1996). ^{14}C is radiogenic and generated in the upper atmosphere. The relatively short

half-life (5568 years) makes it useful in radiometric dating of relatively young

materials (Dickin, 1995), however its low abundance precludes its usefulness as an

isotope tracer of physical and biologic pathways. The ratio of the two stable carbon

isotopes is measured and described in terms of $\delta^{13}C$ defined as;

$$\delta^{13}C = \left[\frac{[R_{Sample}]}{[R_{PDB}]} - 1 \right] * 1000 \qquad (30)$$

where R is the ratio of ^{13}C to ^{12}C, and VPDB refers to the Viennea PeeDee Belemnite

standard, a Cretaceous-aged mollusk (Wang et al., 1998).

The isotopic signature of the DIC of a parcel of water provides information

about the origin and pathway of that parcel. Possible sources of DIC in surface water

include atmospheric exchange, dissolution of subsurface minerals, photosynthesis,

respiration, oxidation of organic matter, and denitrification. The dissolution of

atmospheric CO_2 is driven by the partial pressure of the gas both in the atmosphere

and water. Studies of major river systems suggest that the partial pressure of CO_2 in

water is 10-15 times higher than atmospheric concentrations, which suggests that

rivers are a source of CO_2 degassing (Yang et al., 1996). Studies found the oxidation

of organic matter as the general cause of CO_2 overpressure, with nutrient pollution cited as the cause of increased organic productivity (Yang et al., 1996; Atekwana and Krishnamurthy, 1998). Seasonal variation of more negative values in the winter months and more positive values in the summer months have been observed (Helie et al., 2002).

Two potential sources of groundwater CO_2 result from equilibration with soil gas and dissolution of carbonaceous rocks. A parcel of groundwater equilibrated with soil gas exchange in the root zone would be expected to have a $\delta^{13}C \sim -21‰$ (Bohlke and Denver, 1995). Bolhke and Denver (1995) found this to be the case with surficial Aquia groundwater samples. Suboxic samples taken near the redox transition are less negative (-10‰ to -21‰), reflecting a mixture of limestone dissolution ($CaCO_3$ has $\delta^{13}C \sim 0‰$) and groundwater with a soil gas signature (Bohlke and Denver, 1995).

Surficial processes expected to alter the DIC isotopic signature include atmospheric exchange, photosynthesis, respiration and oxidation of organic material including that caused by denitrification. Exchange with the atmosphere would drive the carbon signature towards atmospheric levels (-8‰) (Wang et al., 1998). As previously stated, this is not expected to be a predominant factor in DIC isotopic values as river systems tend to have higher CO_2 partial pressure than the atmosphere (Yang et al., 1996). Degassing of over pressured DIC should result in ^{13}C enrichment (Atekwana and Krishnamurthy, 1998). Photosynthetic processes uptake $^{12}CO_2$ over its heavier counterpart resulting in an enriched DIC reservoir (Stumm and Morgan, 1996). This discrimination also leads to the significantly depleted signatures in plant matter. The average C3 and C4 isotopic composition are -27‰ and -13‰,

respectively (Wang et al., 1998). Addition of CO_2 from respiration or decay of organic material results in an isotopic depletion of the DIC reservoir (Atekwana and Krishnamurthy, 1998; Yang et al., 1998).

Denitrifying bacteria utilize organic carbon as an electron source for denitrification. The isotopic signature of the produced DIC would be similar to that of the carbon source. In order bacteria to denitrify groundwater, it must come in contact with anoxia. The deep Hornerstown aquifer is known to be anoxic (Bachman et al., 2002). However, based on the calcium to magnesium ratio and 1st-order tributary character it is unlikely that water discharging in the study site has come in contact with the Hornerstown reduced lithologic layer. In the upper reach of the unaltered tributary, the whole stream becomes anoxic resulting from the consumption of bioavailable oxygen. Here nitrate concentrations are extremely low, suggesting bulk denitrification. Denitrifying bacteria utilize NO_3^- as an electron acceptor in their respiratory process (Gerardi, 2002). With measurable decreasing nitrate and increasing in bicarbonate this process would affect the proportion of ^{13}C in the DIC.

On the two winter sampling dates the clearest trends are exhibited. The absence of algae minimizes the number of influencing factors. On each of these dates the ditched tributary shows an enriching trend. The discharging water at the ditched tributary headwaters is slightly less depleted than was measured in the Aquia aquifer (-21‰). This suggests a process, or combination of processes, are either preferentially removing the lighter ^{12}C or contributing a relatively heavier source. Possible processes inducing ^{13}C enrichment include dissolution of atmospheric CO_2, escaping CO_2, and oxidation of organic material. On November 26th the enriching

trend is comparable to that of sample date October 29th (+1.6‰ per 100 m; +1.2‰ per 100 m), however the earlier sample date exhibits overall more negative values. The stepwise lighter values on October 29th are a result of oxidation of organic matter in the channel. Sample date November 26th is further into the winter season when decay is no longer an active process. Thus the measured values are indicative of groundwater delivery. Additionally the colder temperatures would limit further biologic activity. The increasing or decreasing trends of other chemical constituents in the ditched tributary result from chemical gradients in the surficial Aquia aquifer. Bohlke and Denver only measured five carbon isotopic values; therefore it is not clear what type of gradient exists within the aquifer. The results from winter sample dates suggest that a gradient of most negative values in the shallow aquifer getting relatively heavier with depth. Growing algae and other plant material were not observed in the channel on either sample date.

On all other sample dates isotopic values appeared to oscillate around a value of -10‰ in the ditched tributary without any appreciable trends. On each of these three sample dates (July 1st, July 21st, and August 10th) substantial algae was observed in the stream channel. Groundwater discharging to the channel should have an isotopic value of -21‰. Both photosynthesis and equilibration with atmospheric CO_2 would result in enrichment. While it is not clear which factor is dominant based on analytical results, based on theoretical considerations photosynthesis is interpreted as the dominate process. Photosynthesis preferentially removes ^{12}C from surface water and its rate is great than that of atmospheric exchange (Yang et al., 1996).

The unaltered tributary trends are even more difficult to deconvolute. Sample date November 26th exhibit a slightly depleting trend with substantially lighter values than the ditched tributary samples taken from the same date. Sample date July 1st exhibits values more negative than the ditched tributary. Sample date July 21st has slightly lighter values in the uppermost reach and slightly heavier values closer to the confluence, with the average comparable to the ditched tributary values from the same sample date. There is no appreciable trend on sample date August 10th, nor is there an offset from ditched tributary values of the same date. Sample date October 29th exhibits extremely enriched values in the headwaters. This is interpreted as a loss of the lighter ^{12}C through degassing of CO_2. Denitrification produces an excess of DIC overpressure that is relieved through preferential degassing of the lighter isotope.

The location and abundance of algae and other plant material varied both temporally and spatially in this study. No systematic survey was made to estimate the variable location and abundance of plant material. The variability in isotopic values is thought to result from the variability of plant material. This is supported by the clearer trends on the winter sampling dates.

Temporal variation in $\delta^{13}C$ of DIC exhibits relatively lighter values in the winter months and heavier values in the summer months. This suggests that photosynthetic activity results in an overall enrichment. This trend is consistent with other DIC studies (Atekwana and Krishnamurthy, 1998; Yang et al., 1998).

4.3.7 Algae Isotopes

The algae samples analyzed for nitrogen and carbon isotopic compositions exhibited little variation on the two sample dates taken (5.0 ± 2.5‰ and -36.6 ± 2.6‰, respectively). The exception was enrichment in nitrogen isotopic values in the unaltered tributary on October 29th. The substantially heavier nitrogen values in the headwaters of the unaltered tributary suggest nitrogen available for plant growth was enriched. Denitrification would result not only in lower nitrate concentrations, but also heavier ^{15}N in the residual nitrate pool. This heavier nitrogen was incorporated into algae, at these sites. While resources were not available to measure ^{15}N abundances of NO_3 in surface water, the enriched ^{15}N contents of algae at that unaltered sites suggests the denitrification and a shift toward ^{15}N enrichment is in fact occurring.

Chapter 5: Conclusions

The majority of the data presented in this study fit the proposed conceptual model. Anthropogenic contaminants systematically decrease with depth in the Chesterville Branch watershed. Calcium in this region results from the dissolution of dolomite, and is thus anthropogenic in nature. The measured surface water trends of decreasing calcium, magnesium, and nitrate concentrations from headwaters to confluence in the ditched tributary are consistent with dilution by deeper less anthropogenically influenced groundwater (Bohlke and Denver, 1995; Bachman et al., 2002). Bohlke and Denver (1995) did not report an alkalinity gradient; however on each sample date bicarbonate concentrations increased from headwaters to confluence. This suggests that bicarbonate concentration increases with depth in the surficial aquifer.

DIC on each of the summer sample dates oscillated near a value of -10‰ in the ditched tributary. The lack of variability results from the productivity of abundant algae and other plants in the stream. Other studies have found that biologic activity controls the isotopic signature of DIC in the summer months (Yang et al., 1996; Nascimento et al., 1997; Atekwana and Krishnamurthy, 1998; Helie et al., 2002). On the winter sample dates, the proportion of ^{13}C in DIC became greater towards the confluence. Bohlke and Denver did not report an isotopic gradient in the surficial Aquia aquifer (1995); they reported only five δ^{13}C values. The DIC measurements made in the winter months suggest an aquifer gradient with the most depleted δ^{13}C near the surface, with carbon isotopic signature becoming heavier with depth. During the winter months the chemical and isotopic values are most indicative of hydrologic

81

processes void of biologic alteration. Other studies found that in the winter months subsurface geologic controls were most important in determining the isotopic composition of surface water (Yang et al., 1996; Nascimento et al., 1997; Atekwana and Krishnamurthy, 1998; Helie et al., 2002).

Chemical trends along the unaltered tributary do not fit the proposed model as well as those along the ditched tributary. However, deviation from the model is a result of undefined surficial processes as opposed to an alternate flow model. First-order tributaries are understood to access relatively shallow groundwater (Fetter, 1996). Strong vertical hydraulic gradient can exist and as a result relatively deep water can make its way into a stream channel. In this study area, locations of such strong hydraulic gradient have been observed as springs bubbling up within the stream channel (Bohlke and Denver, 1995; Bachman et al., 2002; Ator et al.. 2005; this study). However, chemical analysis of these springs indicate a deeper source within the surficial Aquia but do not access the deeper Hornerstown aquifer. There were no springs observed in the unaltered tributary. Considering the depth to the deeper Hornerstown aquifer (~50 meters), the characteristic shallow flow of 1st-order tributaries, and the lack of springs in the unaltered tributary, it is extremely unlikely that an alternate flow model is possible. It is not plausible that a deeper aquifer would be accessed by a 1st-order tributary lacking a strong vertical hydraulic gradient when other locations in the watershed with a strong vertical hydraulic gradient are not accessing the deeper semi-confined aquifer. Instead the variations and trends in the unaltered tributary are most likely the result of surficial processes.

The unaltered tributary gains relatively shallow groundwater along its reach. The upper two sample sites (NT-100 and NT-75) are extremely stagnant. The decay of plant material in the stream channel consumes all dissolved oxygen, creating anoxic conditions. Nitrate concentrations in these two sites on sample dates July 21st, August 10th, and October 29th are near detection limit suggesting near complete denitrification. The likely electron source is the reduced organic matter abundant in the channel.

$$2NO_3^- + 2CH_2O = N_2 + 2HCO_3^- + 2H_2O \qquad (31)$$

Each mole of nitrate reduced should produce a mole of bicarbonate. The nitrate concentration at all other sites is roughly 1000 μmolar. This suggests that complete denitrification would result in an increase of roughly 1000 μmolar bicarbonate. The bicarbonate concentrations on July 21st, August 10th, and October 29th are roughly 500 μmolar greater than other bicarbonate measurements on those dates. In other words, excess bicarbonate is roughly half that expected by complete denitrification. The concentration of DIC is ultimately driven by the partial pressure of CO_2 in the atmosphere and Henry's gas constant. In the upper reach of the unaltered tributary bicarbonate concentrations are roughly two orders of magnitude greater than would be expected based on atmospheric equilibration. This excess would result in degassing and net loss of CO_2 (Atekwana and Krishnamurthy, 1998; Yang et al., 1998). Thus the slightly lower than expected bicarbonate concentration is consistent with a model of denitrification with a reduced carbon electron source. Nascimento and others (1997) measured the increase in DIC and the shift in $\delta^{13}C$ associated with denitrification. The amount of denitrification is traditionally measured as both the

decrease in nitrate concentration and shift in $\delta^{15}N$ of the remaining nitrate pool (McMahon and Bohlke, 1996; Koba et al., 1997; Hinkle et al, 2001; Bohlke, 2002; Bohlke et al., 2002; Ostrom et al., 2002). The work of Nascimento and others (1997) showed that DIC concentration and shift in $\delta^{13}C$ can also be used to quantify denitrification. The measurements of DIC and $\delta^{13}C$ confirm that denitrification is in fact occurring.

Notably the nitrogen isotopic signature of algae sampled on October 29th in the upper reaches of the unaltered tributary are relatively heavy. The preferential selection of the lighter ^{14}N by denitrifying bacteria has been well established (McMahon and Bohlke, 1996; Koba et al., 1997; Hinkle et al., 2001; Bohlke, 2002; Bohlke et al., 2002; Ostrom et al., 2002; Casciotti et al., 2002). In this case, denitrification in the upper reach of the unaltered tributary leaves the residual nitrate relatively enriched in ^{15}N. This heavy nitrate is then incorporated into the algal material. The average ^{15}N of plant algae sampled (leaving out the anomalous high values) is $+ 4.2 \pm 1.0$ ‰. The values for ^{15}N on October 29th at sites NT-85 and NT-100 are $+ 8.8$ ‰ and $+ 12.4$ ‰, respectively. This suggests that the nitrate available for plant growth after denitrification was relatively enriched.

Calcium concentrations are slightly decreasing from headwater to confluence in the unaltered tributary on each sample date. Surficial calcium is expected to be accompanied with a 1:1 molar ratio of magnesium. Were this the case the slightly decreasing trend could suggest that the unaltered tributary, like the ditched, was being slightly diluted by deeper groundwater along its reach. This, however, is not the case.

As discussed in Chapter 4, the anomalous high magnesium concentrations are observed in sample sites NT-50 and NT-25. It appears as though there is an additional source of magnesium that corresponds to the transition between anoxic and oxic conditions. The abrupt increase in nitrate concentration that corresponds to this transition suggests that groundwater laden with nitrate discharges in the stream channel mixing with the nitrate reduced anoxic water from upstream. At the transition between anoxic and oxic conditions there are manganese oxide coatings on the pebbles. Manganese oxide coatings are known for their role in sorbing large cations, specifically calcium (Evans, 1989). This could account for removal of calcium from the system. However this mechanism addresses the preferential removal of calcium. This is useful to describe the changes in the molar ratio of the two cations; however, it is clear that the anomaly lies with magnesium and not calcium. The calcium concentrations fit the proposed model.

While the redox state of the surface water in the unaltered tributary changes from the headwaters to confluence, this does not affect the solubility character of magnesium or calcium. The solubility of each is not redox dependent.

One possible source of magnesium is the decay of plant material occurring upstream. Magnesium is present in the chlorophyll of plants ($C_{55}H_{72}MgN_4O_5$) (Fenchel et al., 2000). This ratio however would provide 55 times more carbon than magnesium. Magnesium increases roughly 200 μM between two sample sites on the unaltered tributary. Decay of plant material ultimately results in inorganic products. For carbon this would be DIC (Stumm and Morgan, 1996). In order for the increase in magnesium to result from chlorophyll decay, an increase of roughly 11,000 μM

would also result. Were the excess a result of magnesium being released from chlorophyll as plant material decayed there would be a much larger increase in other inorganic products of decay, which is not the case.

Denitrification is commonly linked with a decrease in pH (Bohlke, 2002). In this study there was rather an increase in pH in the upper reaches of the unaltered tributary. While nitrate reduction has been the focus of this study because of the implications to algal growth, both in the stream and at downstream estuary sites, it is not the dominant process of the system. Conditions favorable to denitrification developed in the stagnant upper reaches of the unaltered tributary, and thus nitrate reduction occurred. However, the dominant processes are likely related to the decay of plant material abundant in the stream channel, rather than a dissolved component. The pH of decaying material varies substantially based on conditions.

The trends in each of the studied tributaries are distinct from one another. In addition, the chemical composition at each of the headwater sample sites is substantially different. There are two primary factors influencing this difference; 1) the stagnation of the unaltered tributaries contributes to surface water alteration, and 2) the geomorphology of each tributary results in access of different vertical location of the surficial aquifer.

Notably the largest variation in headwater concentrations are in nitrate and bicarbonate. In the ditched tributary nitrate from the uppermost portion of the aquifer is delivered to the stream and promptly transported to downstream sites as a result of the relatively steeper gradient induced by ditching. On the other hand, groundwater delivered to the headwaters of the unaltered tributary remains quite stagnant. Anoxia

results in reduction of nitrate and production of bicarbonate, accounting for the variation in these components between the two tributaries. Notably, the variation between the adjacent 1st-order tributaries persists during the winter months. In stream processing is thought to be greatest at relatively high flow rates. In this case, flow rates were not measurable suggesting the differences are a result of varying sources; the ditched tributary accesses relatively deeper water and the unaltered tributary accesses relatively shallower younger groundwater.

Ditching of agricultural tributaries in the Eastern shore is to enhance drainage from the fields. Ditching ultimately lowers the water table by accessing and draining deeper portions of the surficial aquifer (Fetter, 1996). Each sub-watershed in this study has a similar drainage basin size. However, alteration of the ditched tributary results in a higher discharge. Discharge in the unaltered tributary decreases as the water table lowers. As water table declines, the length of permanent unaltered tributary also decreases. The result is that the headwaters of the ditched tributary accesses and drains a shallow portion of the Aquia aquifer that the unaltered tributary never accesses.

The control of nitrate flux from first order tributaries to downstream sites is the primary focus of this work. Reducing nitrate flux plays an integral role in minimizing the eutrophication problem of estuaries and bays, in this case the Chesapeake Bay. Models have been developed that link the loss of nitrate statistically to channel size (Smith et al., 1997; Preston and Brakebill, 1999). The work presented in this study shows that geomorphologic character of similar sized stream channels is an important parameter in determining nitrate transport and flux.

Peterson and others (2001) studied the removal of nitrate in small headwater streams. They found that an increase in water interaction with soil was important in denitrification. In Chesterville Branch, water interaction was maximized in the unaltered tributary, and minimized due to an increased gradient in the ditched tributary.

The research surrounding nitrate transformations in surface water systems ultimately seeks to decrease the flux of nitrate to downstream sites. Pinay and others (2002) described three parameters that can be used to manage nitrate concentration: 1) understanding the mode of nitrogen delivery to the stream, 2) increase the contact between water and soil, and 3) understanding the role of natural floods and droughts to nitrate flux. Each of these parameters affects the Chesterville Branch nitrate flux.

Pinay and others (2002) describe the mode of nitrogen delivery to the stream in terms of geomorphology. They found that channel incision resulted in a source of sediment and nutrients, whereas prior to alteration that same sediment intact resulted in a sink for nutrients. The lack of nitrate reduction in the ditched tributary is likely related to such processes.

Nitrate from both the uppermost portion and deeper portions of the aquifer are being delivered to the stream. Nitrate concentrations in the deeper aquifer are a result of fertilizer application over twenty years ago. However the shallowest flow paths of groundwater, which are notably the highest in nitrate concentration, result from recent applications. Elmi and others (2002) showed that nitrate being delivered from this shallowest flow path can be minimized by managing both fertilizer application rates and water table level. In Chesterville Branch where ditching has resulted in a

drawdown of the water table, nitrate delivery to the stream could be minimized by raising water table. This would ultimately increase the residence time of surface water, and thereby increase the interaction between water and soil. Incentive payments could be offered by the government to encourage such practices. Similar programs have been successful in promoting conversion of land directly adjacent to agricultural streams into riparian forested buffers (Bohlke, 2002).

Finally, understanding the role of natural floods and droughts to nitrate transformations will help to further model nitrate flux. The depth to the water table is more strongly influenced by climate controls rather than geomorphology (Burt et al., 2002; Clement et al., 2003). Relatively higher discharge in a given stream channel reduces the interaction of water and sediment, thereby decreasing the removal of nitrate. Therefore high water years result larger flux of nitrate to downstream sites. The climatic conditions over the course of this study were relatively wet (Ator et al., 2005). This would suggest that nitrate removal was lower than would be expected in lower water years. However, even with relatively wet conditions, there was a measurable difference in nitrate flux between the two adjacent first order tributaries. Pulse of nitrate delivered during actual storm events also affect total flux of nitrate to downstream sites. This study was conducted at base flow and thus there are no quantifiable results related to storm events. However, the ditching in Chesterville Branch lowers the water table. This would result in a larger unsaturated zone. During a storm event, nitrate that had accumulated in that unsaturated zone would be flushed out into the stream.

Ultimately the implications of this study are that physical alteration of a stream channel changes the ability to transform chemical constituents, namely nitrate. Ditching accesses older groundwater which may be more dilute with respect to anthropogenic contaminants, but ultimately ditching inhibits the natural attenuation of nitrate through denitrification. While this study considered only a relatively small geographic location, first order tributaries comprise a large portion of waterways in the Eastern shore (Figures 1 and 2). Nitrate removal is most effective in smaller stream channels. As tributaries converge to form larger channels interaction between surface water and soil decreases, and thus potential for nitrate removal does as well. Management and reduction of nitrate is best aimed at first order tributaries. The results of this study confirm those of Helie and others (2002); relatively higher water table with respect to channel depth enhances the removal of nitrate as seen in the unaltered tributary.

In order to more accurately predict flux of nitrate to downstream sites, the input parameters of predictive models should include geomorphology of stream channels and relative depth to the water table. By including such parameters in predictive models, not only would the ability of those models to accurately predict nitrate flux improve, but also those locations of greatest nitrate contributions could be better identified. With those sites identified, management and resources could be focused on reducing nitrate flux from those sites of highest contribution.

Appendices

Appendix A. Data

Sample 11/26/2003	pH	Temp °C	HCO₃⁻ mg/L	NO₃⁻ μM	Mg μM	Ca μM	Ca:Mg	δ¹³C ‰, VPDB	Na μM
MS-200-A	6.22	9.4		751	304.6	451.2	1.464	-14.7	0.2379
MS-200-B						440.8		-14.4	0.1486
MS-100-A	6.13	10.5		804	349.7	482.0	1.382		0.1486
MS-100-B						484.5			0.1614
MS-0-A	6.09	10.8		814	324.2	425.2	1.271	-14.1	0.1444
MS-0-B						399.2		-14.0	0.1402
NT-0-A	6.70	7.4		245	588.1	753.7	1.264	-10.2	0.4291
NT-0-B						732.6		-10.2	0.4248
NT-25-A	6.82	7.1		183	611.6	766.0	1.246		0.4448
NT-25-B						758.2			0.4554
NT-50-A	6.90	6.9		132	566.7	771.2	1.363	-9.8	0.3988
NT-50-B						773.8		-8.9	0.4873
NT-100-A	7.08	6.7		60	384.0	799.8	2.093	-9.2	0.5120
NT-100-B						807.6		-10.0	0.5191
DT-0-A	6.00	11.0		874	346.1	335.9	0.952	-14.3	0.1215
DT-0-B						323.3		-14.1	0.1095
DT-25-A	6.01	11.8		884	344.3	338.4	0.990	-14.3	0.1119
DT-25-B						343.5		-13.9	0.1143
DT-50-A	5.99	11.7		884	316.7	421.3	1.330	-14.7	0.1143
DT-50-B								-13.8	0.1143
DT-100-A	5.86	11.8		1013	384.0	394.1	1.026	-15.0	0.1143
DT-100-B								-14.8	0.1215
DT-200-A	5.77	12.0		987	387.6	419.0	1.078	-15.2	0.1167
DT-200-B						416.5		-15.1	0.1215
DT-300-A	5.70	12.3		1076	384.0	468.2	1.219	-15.7	0.0943
DT-300-B								-16.1	0.0943
DT-400-A	5.59	12.3		1165	418.5	500.3	1.195	-17.0	0.0924
DT-400-B						416.7	492.9	1.183	-16.3	0.0904
DT-500-A	5.53	12.0		1182	447.6	391.6	0.875	-18.1	0.0963
DT-500-B								-18.4	0.0924
DT-525-A	5.52	12.0		1161	490.6	409.0	0.836	-18.5	0.0943
DT-525-B						411.5		-18.6	0.1218

Sample 5/5/2004	pH	Temp °C	HCO$_3^-$ mg/L	NO$_3^-$ μM	Mg μM	Ca μM	Ca:Mg	δ^{13}C ‰, VPDB	Na μM
MS-0-A	6.38	18.2	20.2	783					
MS-0-1					235.9	364.0	0.668		
MS-0-2						342.8			
DT-0-A	6.00	18.4	20.2	787					
DT-0-1					304.6	446.1	0.681		
DT-0-2						448.5			
NT-0-A	6.56	18.7	93.1	332					
NT-0-1					359.9	488.4	0.735		
NT-0-2						490.7			
DT-A-U	5.76	18.7	11.6	950					
DT-U-1					349.2	420.3	0.828		
DT-U-2						422.7			
MS-A-D	6.10	18.4	28.4	745					
MS-1-D					292.1	434.4	0.663		
MS-2-D						446.1			

Sample 7/1/2004	pH	Temp °C	HCO₃⁻ mg/L	NO₃⁻ µM	Mg µM	Ca µM	Ca:Mg	δ¹³C ‰, VPDB	Na µM
MS-150-1	6.19	18.2	17.3	662	260.8	398.0	1.526	-11.2	
MS-150-2					264.6	393.4	1.487		0.1653
MS-100-1	6.27	18.4	8.0	853	345.7	569.1	1.646	-8.4	
MS100-2					334.4	557.7	1.668		0.1943
MS-0-1	6.04	18.5	15.8	771	268.4	395.7	1.474	-9.1	0.1042
MS-0-2					272.1	386.6	1.420		0.1061
NT-100-1			26.0	486	242.0	457.3	1.890	-10.0	0.1035
NT-100-2					243.9	448.2	1.838		0.1001
NT-75-2			16.4	532	249.5	434.5	1.741	-10.2	0.1018
NT-75-1					243.9	448.2	1.838		0.1035
NT-50-1			29.2	538	251.4	434.5	1.728	-12.0	0.0967
NT-50-2					245.7	411.7	1.675		0.0984
NT-25-1			29.6	525	251.4	445.9	1.774	-12.1	
NT-25-2					245.7	434.5	1.768		0.0863
NT-0-1	6.34	21.6	27.6	552	251.4	439.0	1.746	-12.8	0.0943
NT-0-2					253.3	413.9	1.634		0.0842
DT-300-1			17.0	783	286.8	372.4	1.299	-10.4	0.1365
DT-300-2					283.1	344.3	1.216		0.1304
DT-250-1			14.5	764				-11.1	0.1258
DT-250-2									0.1319
DT-200-1			16.5	812	292.3	386.5	1.322	-9.6	0.1166
DT-200-2					290.5	391.2	1.347		0.1212
DT-150-1			13.5	847	299.7	417.0	1.391	-9.5	0.1182
DT-150-2					296.0	414.7	1.401		0.1166
DT-100-1			15.3	853	299.7	353.6	1.180	-10.0	
DT-100-2					299.7	341.9	1.141		0.1173
DT 75-1			8.5	871	305.3	384.1	1.258	-10.2	0.1294
DT-75-2					301.6	379.5	1.258		0.1122
DT-50-1			11.3	874	301.6	433.4	1.437	-8.8	0.1122
DT-50-2					301.6	421.7	1.398		0.1122
DT-25-1			13.3	896	297.9	438.1	1.471	-8.7	0.1122
DT-25-2					299.7	431.1	1.438		0.1087
DT-0-1	6.03	18.6	14.2	860	288.6	421.7	1.461	-10.6	0.1087
DT-0-2					283.1	405.3	1.432		0.1122

Sample 7/21/2004	pH	Temp °C	HCO$_3^-$ mg/L	NO$_3^-$ μM	Mg μM	Ca μM	Ca:Mg	δ^{13}C ‰, VPDB	Na μM
MS-150-1	5.64	17.7	17.0	806	349.5	338.4	0.968	-12.1	0.1121
MS-150-2					329.5	311.5	0.945		0.1105
MS-100-1	5.52	18.2	17.8	801	332.0	374.2	1.127	-11.1	0.1136
MS100-2					339.5	342.9	1.010		0.1075
MS-0-1	5.44	19.5	14.5	806	357.0	329.4	0.923	-11.0	0.1121
MS-0-2					354.5	302.5	0.853		0.1350
NT-0-1	5.16	19.2	11.2	829	409.5	226.4	0.553	-11.7	0.1182
NT-0-2					397.0	208.4	0.525		0.1182
NT-25-1			13.9	854	562.0	262.2	0.466	-12.6	0.1105
NT-25-2					545.5	231.8	0.425		0.1090
NT-50-1	5.21	25.2	13.6	895	585.2	272.3	0.465	-7.5	0.0910
NT-50-2					601.8	252.0	0.419		0.0925
NT-75-1			50.0	5	255.6	418.7	1.638		0.1866
NT-75-2					251.2	408.6	1.627		0.1721
NT-100-1	5.96	30.5	52.4	0	268.9	444.0	1.651	-9.8	0.1605
NT-100-2					271.1	408.6	1.507		0.1576
DT-0-1	5.45	19.5	15.3	805	370.4	396.0	1.069	-9.9	0.1040
DT-0-2					367.9	379.2	1.031		0.1026
DT-25-1			16.3	826	380.4	211.1	0.555	-11.1	0.1069
DT-25-2					377.9	222.3	0.588		0.1040
DT-50-1	5.49	21.5	15.0	824	377.9	396.0	1.048	-10.2	0.0968
DT-50-2					372.9	373.6	1.002		0.1069
DT 75-1			15.8	842	392.9	390.4	0.994	-10.2	0.1011
DT-75-2					375.4	390.4	1.040		0.1069
DT-100-1	5.52	21.9	15.5	978	380.4	356.8	0.938		0.1011
DT-100-2					370.4	351.2	0.948		0.0997
DT-150-1			11.1	1115	405.3	356.8	0.880	-10.9	0.1040
DT-150-2					412.8	351.2	0.851		0.1055
DT-200-1	4.90	21.7	10.4	1009	415.3	356.8	0.859	-10.9	0.0984
DT-200-2					415.3	340.0	0.819		0.0984
DT-250-1			9.0	975	402.8	373.6	0.927	-10.9	0.0955
DT-250-2					400.3	356.8	0.891		0.0941
DT-300-1	5.04	22.1	3.5	1119	427.8	289.5	0.677	-9.8	0.0984
DT-300-2					425.3	261.5	0.615		0.0941

Sample 8/10/2004	pH	Temp °C	HCO₃⁻ mg/L	NO₃⁻ μM	Mg μM	Ca μM	Ca:Mg	δ¹³C ‰, VPDB	Na μM
MS-150-1	5.04	22.1	17.0	802	289.8	418.1	1.443	-7.0	0.1027
MS-150-2					287.8	398.4	1.384		0.0984
MS-100-1			18.0	797	287.8	398.4	1.384	-6.8	0.0004
MS100-2					289.8	388.6	1.341		0.1027
MS-0-1	5.99	18.3	17.8	814	311.9	398.4	1.278	-6.2	0.1070
MS-0-2					299.9	388.6	1.296		0.0998
NT-0-1	5.53	18.1	8.7	880	370.0	280.0	0.757	-7.8	0.1915
NT-0-2					361.9	270.2	0.746		0.1901
NT-25-1			17.0	839	519.5	272.6	0.525	-4.2	0.0082
NT-25-2					516.6	265.2	0.513		0.0755
NT-50-1	5.81	19.5	15.5	871	510.6	322.0	0.630	-2.3	0.0697
NT-50-2					510.6	299.8	0.587		0.0783
NT-75-1			47.5	1	277.8	403.3	1.452	-6.0	0.1172
NT-75-2					261.8	393.5	1.503		0.0332
NT-100-1	6.34	21.8	45.8	2	257.8	331.8	1.287	-7.9	0.1130
NT-100-2					249.8	317.0	1.269		0.0836
DT-0-1	5.96	18.4	15.9	780	302.7	285.6	0.944	-7.9	0.1018
DT-0-2					300.7				0.0584
DT-25-1			18.0	821	300.7	405.4	1.348	-7.7	0.1074
DT-25-2					296.8	387.6	1.306		0.0990
DT-50-1	6.07	19.3	16.3	789	306.6	382.5	1.247	-6.5	0.1074
DT-50-2					300.7	385.1	1.280		0.0290
DT-100-1			20.5	810	302.7			-5.3	0.0542
DT-100-2					294.8	341.7	1.159		0.0948
DT-150-1				906	330.2	392.7	1.189	-8.5	0.0584
DT-150-2					324.3	362.1	1.116		0.1018
DT-200-1	5.70	19.5	13.6	980	338.1	385.1	1.139	-7.7	0.1074
DT-200-2					326.3	367.2	1.125		0.1060
DT-250-1					326.3	313.7	0.961	-8.2	0.0500
DT-250-2					318.4	288.2	0.905		0.0416
DT-300-1	5.55	18.8	10.3	1008	342.1	341.7	0.999	-9.5	0.1058
DT-300-2					330.2	308.6	0.934		0.1001

Sample 10/29/2004	pH	Temp °C	HCO$_3^-$ mg/L	NO$_3^-$ µM	Mg µM	Ca µM	Ca:Mg	δ^{13}C ‰, VPDB	Na µM
MS-150-2					286.2	460.4	1.609		0.0915
MS-100-1	5.65	13.3	15.9	897	294.1	453.9	1.544	-14.8	0.0944
MS100-2					288.1	457.2	1.587		0.0915
MS-0-1	5.78	14.1	14.0	891	303.9	444.1	1.461	-13.5	0.1001
MS-0-2					300.0	437.5	1.459		0.1058
NT-0-1	5.30	13.3	8.1	963	397.1	359.0	0.904	-15.7	0.1044
NT-0-2					397.1	365.5	0.921		0.0929
NT-25-1			11.0	1003	533.4	342.6	0.642	-15.7	
NT-25-2					530.5	339.4	0.640		0.0915
NT-50-1	5.48	13.6	10.9	1012	524.5	329.5	0.628	-13.1	0.0743
NT-75-1			44.0	3	309.9	434.2	1.401		0.0958
NT-75-2					307.9	434.2	1.410		0.1001
NT-100-1	6.71	13.1	42.8	17	280.2	431.0	1.538	-4.2	0.0915
NT-100-2					274.3	417.9	1.523		0.1001
DT-0-1	5.74	14.2	13.6	861	317.8	427.7	1.346	-11.4	
DT-0-2					313.8	424.4	1.353		
DT-25-1			13.9	916	313.2	412.6	1.317	-10.8	
DT-25-2					315.2	418.6	1.328		
DT-50-1			15.0	910	311.2	418.6	1.345	-11.0	
DT-50-2					315.2	427.8	1.357		
DT 75-1	6.21	14.6	13.8	841	315.2	430.8	1.367	-11.1	
DT-75-2					317.2	430.8	1.358		
DT-100-1			14.4	920	313.2	433.9	1.385	-12.3	
DT-100-2					315.2	440.0	1.396		
DT-150-1	5.94	14.7	9.6	993	335.3	421.7	1.258	-13.0	
DT-150-2					339.3	418.6	1.234		
DT-200-1	5.85	14.7	8.4	1000	335.3	424.7	1.267	-13.2	
DT-200-2					339.3	409.5	1.207		
DT-250-1	5.86	14.6	8.2	1011	333.2	430.8	1.293	-13.2	
DT-250-2					337.3				
DT-300-1	5.73	14.6	6.2	1050	347.3	412.6	1.188	-14.9	
DT-300-2					353.3	430.8	1.219		

Appendix B
Error Calculations

Distance

Distances between sampling sites were determined by using a metric tape measure. The uncertainty of measurement is on the order of ± 1 meter. Usually the length of the error bars implies the uncertainty in the x-direction. In the case of the figures generated for this study, the length of the error bars would be much smaller than are shown. A wider error bar was used to accentuate the error in concentrations of various chemical constituents (y-axis) and do not represent error in distance measurements.

pH

pH values were determined using a HACH ion probe instrument. The pH meter was calibrated using standard reagents with pH values of 4.01, 7.00, and 10.01. The instrument automatically generates a calibration curve and corrects for variations in temperature. Ten repeat measurements were taken on the same river site to determine the uncertainty of the instrument. The average value was 7.500 ± 0.079 pH units, or a 1σ relative uncertainty of ± 1.1%.

Temperature

Temperature values were taken from the pH probe for consistency. In the instrument manual the instrument claims an accuracy of ± 0.3 °C. There is not an option for calibrating the temperature sensor on the instrument. Ten repeat measurements were taken at the same river site to determine the uncertainty of the instrument. The average value was 17.63 ± 0.05 °C, or a relative uncertainty of ±

97

0.3%. Error bars aren't shown on temperature graphs. The error is smaller than the symbol size selected.

Atomic Absorption Spectrophotometer

Calcium

Calcium uncertainty was determined by running the same sample seven times. Each sample was diluted by the same proportions as field samples to ensure any error with dilution is also accounted. Average calcium concentration was 15.11 ± 0.17 mg/L. This represents a 1σ of $\pm 1.1\%$ relative uncertainty.

Magnesium

Magnesium uncertainty was determined by running the same sample seven times. Each sample was diluted by the same proportions as field samples to ensure any error with dilution is also accounted for. Average magnesium concentration was 6.66 ± 0.14 mg/L. This represents a $\pm 2.2\%$ uncertainty.

Calcium to Magnesium Ratio

The error of a quotient is determined through the equation

$$\frac{E_{Ca:Mg}}{Ca:Mg} = \sqrt{\left(\frac{E_{Ca}}{Ca}\right)^2 + \left(\frac{E_{Mg}}{Mg}\right)^2}$$

When solved, the relative error for the calcium to magnesium ratio is $\pm 2.5\%$

Sodium

Sodium uncertainty was calculated using the standard values run as samples after instrument calibration. For 36 standards the 1σ relative uncertainty is $\pm 3.6\%$.

Ion Chromatography

Nitrate concentrations were obtained using an Ion Chromatograph at Horn Point Laboratory, an affiliate of University of Maryland. Uncertainty was determined by periodically running standards along with the sample run. The majority of nitrate samples analyzed in this study required a high range nitrate method (25-400 μM). The 1σ relative uncertainty of these samples is ± 3.2%. Samples NT-75-7-21-04, NT-100-7-21-04, NT-75-8-10-04, NT-100-8-10-04, NT-75-10-29-04, and NT-100-10-29-04 required the low nitrate method (0-10 μM). The 1-σ relative uncertainty of these measurements was ± 0.17%.

Alkalinity

Ten duplicate samples were titrated to determine the uncertainty of this method. The average value measured was 33.7 ± 1.5mg/L, or a relative uncertainty of 4.4%.

Isotopic Values of Dissolved Inorganic Carbon

Seawater was used as a standard for DIC measurements. The seawater was calibrated using a laboratory solid carbonate standard. Seawater was used as a reference so that the standard and sample were in the same matrix; water. The solid carbonate requires a slightly different preparation described in the main text of this document. Between 150 and 200 μg of solid carbonate was put into a vial. The vial was then flushed for ninety seconds with inert helium. Through the septum 500 μL of 85% phosphoric acid was delivered and left to react for five minutes in a heated sample tray (40 °C). The headspace was then analyzed using the same procedure as for seawater and liquid samples. Reproducibility of the seawater standard was quite

99

good with a 1σ uncertainty of ± 1.5% (n= 20). However the 1σ uncertainty in the house solid carbonate standard measurements was ± 6.6% (n=5). The solid carbonate was used to calibrate the seawater standard thus the certainty of all samples depends on the uncertainty of the solid carbonate. The average house carbonate is 1.000 ± 0.070 ‰ and the average seawater standard value is -5.53 ± 0.36 ‰.

Plant Algae Isotopes

Absolute uncertainty in nitrogen and carbon isotopic values range from ± 0.04-0.09 ‰ and ± 0.03-0.16 ‰, respectively (n =16). These were determined for each set of sample runs by quantifying deviation of the standard Urea. Individual uncertainties are included in Table 3 in the main text of this document.

Appendix C

Trendline Equations

Table C-1. Trendline equations of pH measurements

Date	Natural Tributary		Ditched Tributary	
	Equation	r^2	Equation	r^2
11-26-03	y = -0.0037x + 6.7118	0.9948	y = 0.0019x + 6.0142	0.9424
7-21-04	y = -0.008x + 5.0425	0.7971	y = 0.002x + 5.5345	0.6679
8-10-04	y = -0.0081x + 5.4876	0.9694	y = 0.0016x + 6.0437	0.8882
10-29-04	y = -0.0196x + 5.1773	0.9537	y = 0.0005x + 5.9678	0.0956

Table C-2. Trendline equations of temperature measurements

Date	Natural Tributary		Ditched Tributary	
	Equation	r^2	Equation	r^2
11-26-03	y = 0.0067x + 7.3203	0.9291	y = -0.0024x + 11.568	0.4199
7-21-04	y = -0.1131x + 19.307	0.9987	y = -0.0063x + 20.524	0.5151
8-10-04	y = -0.037x + 17.947	0.9808	y = -0.001x + 18.867	0.0718
10-29-04	y = 0.0037x + 13.457	0.3167	y = -0.0011x + 14.39	0.4225

Table C-3. Trendline equations of alkalinity measurements

Date	Natural Tributary		Ditched Tributary	
	Equation	r^2	Equation	r^2
7-1-04	y = 1.0764x + 476.02	0.2288	y = -0.2376x + 195.63	0.3308
7-21-04	y = -7.7764x + 73.525	0.7948	y = 0.6347x + 284.88	0.8793
8-10-04	y = -6.87x + 97.232	0.8178	y = 0.3703x + 300.07	0.5506
10-29-04	y = -6.7197x + 46.729	0.7800	y = 0.4856x + 249.8	0.8627

Table C-4. Trendline equations for calcium concentrations.

Date	Natural Tributary		Ditched Tributary	
	Equation	r^2	Equation	r^2
11-26-03	y = -0.5925x + 744.44	0.9246	y = -0.3069x + 365.77	0.3394
7-1-04	y = -0.2146x + 426.02	0.2969	y = 0.1876x + 417.13	0.3264
7-21-04	y = -2.3398x + 196.26	0.8585	y = 0.0812x + 352.22	0.0206
8-10-04	y = -0.9134x + 269.85	0.4725	y = 0.1563x + 376.24	0.1677
10-29-04	y = -0.8715x + 340.11	0.5908	y = 0.0076x + 425.27	0.0081

Table C-5. Trendline equations for magnesium concentrations.

Date	Natural Tributary		Ditched Tributary	
	Equation	r^2	Equation	r^2
11-26-03	y = 2.207x + 634.18	0.8191	y = -0.4849x + 328.14	0.8847
7-1-04	y = 0.0831x + 251.97	0.5916	y = 0.0313x + 298.97	0.1819
7-21-04	y = 2.2711x + 528.37	0.3265	y = -0.1795x + 369.91	0.7909
8-10-04	y = 1.8935x + 478.36	0.3473	y = -0.1286x + 297.83	0.7257
10-29-04	y = 1.8537x + 487.71	0.4426	y = -0.1239x + 310.12	0.8278

Table C-6. Trendline equations for Calcium to Magnesium ratio

Date	Natural Tributary		Ditched Tributary	
	Equation	r^2	Equation	r^2
11-26-03	y = -0.0087x + 1.11	0.8455	y = 0.0004x + 1.1253	0.0692
7-1-04	y = -0.0015x + 1.69	0.4987	y = 0.0005x + 1.3975	0.2168
7-21-04	y = -0.0131x + 0.2733	0.6905	y = 0.0006x + 0.948	0.1274
8-10-04	y = -0.0081x + 0.5241	0.5578	y = 0.0009x + 1.2569	0.4566
10-29-04	y = -0.008x + 0.6666	0.6349	y = 0.0005x + 1.3695	0.6049

Table C-7. Trendline equations for nitrate concentrations.

Date	Natural Tributary		Ditched Tributary	
	Equation	r^2	Equation	r^2
11-26-03	y = 1.8176x + 234.64	0.9813	y = -1.1556x + 877.44	0.8949
7-1-04	y = 0.5044x + 551.73	0.636	y = 0.3909x + 889.95	0.8457
7-21-04	y = 10.037x + 1018.5	0.7119	y = -0.9918x + 816.92	0.687
8-10-04	y = 10.385x + 1038	0.7546	y = -0.8344x + 772.22	0.8963
10-29-04	y = 11.579x + 1178.8	0.7211	y = -0.621x + 865.2	0.8072

Table C-8. Trendline equations for dissolved inorganic carbon isotopic values.

Date	Natural Tributary		Ditched Tributary	
	Equation	r^2	Equation	r^2
11-26-03	y = -0.0058x - 10.007	0.2276	y = 0.0163x - 13.691	0.9521
7-1-04	y = 0.0025x - 12.077	0.005	y = 0.0036x - 9.4168	0.2057
7-21-04	y = -0.027x - 11.572	0.2669	y = 0.0003x - 10.447	0.003
8-10-04	y = 0.008x - 5.2475	0.0173	y = 0.0062x - 6.8193	0.2774
10-29-04	y = -0.1211x - 17.473	0.9011	y = 0.0123x - 10.747	0.8741

Bibliography

Alexander, R.B., Smith, R.A., and Schwarz, G.E. (2000) Effect of stream channel size on the delivery of nitrogen to the Gulf of Mexico. *Nature* **403**, 758-761.

Atekwana, E.A., and Krishnamurthy, R.V. (1998) Seasonal variations of dissolved inorganic carbon and $\delta^{13}C$ of surface waters: application of a modified gas evolution technique. *Journal of Hydrology*, **205**, 265-278.

Ator, S.W., Denver, J.M., and Brayton, M.J., (2005) Hydrologic and Geochemical Controls on Pesticide and Nutrient Tranpsort to Two Streams on the Delmarva Peninsula. **USGS Scientific Investigations Report 2004-5051**.

Bachman, L.J., Krantz, D.E., and Bohlke (2002) Hydrogeologic Framework, Ground Water Geochemistry, and Assessment of Nitrogen Yield from Base Flow in Two Agricultural Watersheds, Kent County, Maryland. U.S. Environmental Protection Agency, **EPA/600/R-02/008**.

Bencala, K.E. (2000) Hyporheic zone hydrological processes: *Hydrological Processes*, **14**, 2797-2798.

Boggs, S. (1995) Principles of Sedimentology and Stratigraphy. 2nd Edition. Prentice Hall Inc. Upper Saddle River, New Jersey.

Bolhke, J.K., and Denver J.M., (1995) Combined use of groundwater dating, chemical, and isotopic analyses to resolve the history and fate of nitrate contamination in two agricultural watersheds, Atlantic coastal plain, Maryland. *Water Resources Research*, **31(9),** 2319-2339.

Bolhke, J.K. (2002) Groundwater recharge and agricultural contamination. *Hydrogeology Journal*, **10**, 153-179.

Bolhke, J.K., Wanty, R., Tuttle, M., Delin, G., and Landon, M. (2002) Denitrification in the recharge area and discharge area of a transient agricultural nitrate plume in a glacial outwash sand aquifer, Minnesota, *Water Resources Research*, **38(7)**, 10.

Burt, T.P., Pinay, G., Matheson, F.E., Haycock, N.E., Butturini, A., Clement, J.C., Danielescu,S., Dowrick, D.J., Hefting, M.M., Hillbricht-Ilkowska, A., and Maitre V. (2002) Water table fluctuations in the riparian zone: comparative results from a pan-European experiment. *J of Hydrology,* **265**, 129-148

Caraco, N.F., and Cole, J.J., (1999) Human impact on nitrate export: An analysis using major world rivers. *Ambio*. **28 (2),** 167-170.

Casciotti, K.L., Sigman, D.M., Galanter Hastings, M., Bohlke, J.K., and Hilkert, A., (2002) Measurement of the Oxygen Isotopic Composition of Nitrate in Seawater and Freshwater Using the Denitrifier Method, *Analytical Chemistry*, **74**, 4905-4912.

Chang, C.Y., Kendall, C., Silva, S.R., Battaglin, W.A., and Campbell, D.H. (2002) Nitrate stable isotopes: tools for determining nitrate sources among different land uses in the Mississippi River Basin, *Can. J. Fish. Aquat. Sci.,* **59**, 1874 1885.

Clement, J.C., Aquilina, L., Bour, O., Plaine, K., Burt, T.P., and Pinay G. (2003) Hydrological flowpaths and nitrate removal rates within a riparian floodplain along a fourth-order stream in Brittany (France). *Hydrological Processes.* **17**, 1177-1195.

Dickin, A.P. (1995) *Radiogenic Isotope Geology*. Cambridge University Press. Cambridge, UK

Dunkle S.A., Plummer, L.N., Busenberg, Eurybiades, Phillips, P.J., Denver, J.M., Hamilton, P.A., Michel, R.I., and Coplen, T.B. (1993), Chlorofluorocarbons (CCl_3F and CCl_2F_2) as dating tools and hydrologic tracers in shallow groundwater of the Delmarva Peninsula, Atlantic Coastal Plain, Unites States: *Water Resources Research*, **29(12),** 3837-3860.

Evans, L.J., (1989) Chemistry of metal retention by soils. *Environmental Science and Technology*, **23(9)**, 1046-1056.

Fenchel, T., King, G.M., and Blackburn, T.H., (2000) *Bacterial Biogeochemistry: The Ecophysiology of Mineral Cycling*. Academic Press, San Diego, California.

Fetter, C.W. (1994) *Applied Hydrogeology*. Third Edition. Prentice-Hall Inc., Upper Saddle River, New Jersey.

Focazio, M.J., Plummer, L.N., Bohlke, J.K., Busenberg, E., Bachmen, L.J., and Powars, D.S., (1998) Preliminary Estimates of Residence Times and Apparent Ages of Ground Water in the Chesapeake Bay Watershed, and Water-Quality Data From a Survey of Springs. **USGS Water-Resources Investigations Report 97-4225**.

Fuller, C.C., and Harvey, J.W. (2000) Reactive Uptake of Trace Metals in the Hyporheic Zone of a Mining-Contaminated Stream, Pinal Creek, Arizona: *Environmental Science and Technology*, **34(7),** 1150-1155.

Gerardi, M.H. (2002) Nitrification and Denitrification in the Activated Sludge Process. WileyInterscience. New York.

Hantush, M.M., and Cruz, J. (1999) Hydrogeologic Foundations in Support of Ecosystem Restoration: Base-flow Loadings of Nitrate in Mid-Atlantic Agricultural Watersheds. U.S. Environmental Protection Agency. **EPA/600/R-99/104.**

Harvey, J.W. and Bencala, K.E., (1993) The effect of streambed topography on surface subsurface water exchange in mountain catchments. *Water Resources Research*. **29(1)**, 89-98.

Helie, J.F., Hillaire-Marcel, C., and Rondeau, B. (2002) Seasonal changes in the sources and fluxes of dissolved inorganic carbon through the St. Lawrence River – isotopic and chemical constraints. *Chemical Geology*. **186**, 117-138.

Hinkle, S.R., Duff, J.H., Triska, F.J., Laenen, A., Gates, E.B., Bencala, K.E., Wentz, D.A., and Silva, S.R. (2001) Linking hyporheic flow and nitrogen cycling near the Willamette River– a large river in Oregon, USA. *J of Hydrology* **244**, 157-180.

Howarth, R.W., Billen, G., Swaney, D., Townsend, A., Jaworski, N., Lajtha, K., Downing, J.A., Elmgren, R., Caraco, N., Jordan, T., Berendse, F., Freney, J., Kudeyarov, V., Murdoch, P., and Zhu, Z.L., (1996) Regional nitrogen budgets and riverine N&P fluxes for the drainages to the North Atlantic Ocean: Natural and human influences. *Biogeochemistry*. **35 (1)**, 75-139.

Jones, J.B., and Holmes, R.M. (1996) Surface-subsurface interactions in stream ecosystems: *TREE*, **11(6),** 239-242.

Koba, K., Tokuchi, N., Wada, E., Nakajima, T., and Iwatsubo, G., (1997) Intermittent denitrification: The application of a ^{15}N natural abundance method to a forested ecosystem. *Geochimica et Cosmochimica Acta*. **61(23)**, 5043-5050.

Konohira, E., Yoh, M., Kubota, J., Yagi, K, and Akiyma, H. (2001) Effects of riparian denitrification on stream nitrate-evidence from isotope analysis and extreme nitrate leaching during rainfall. *Water, Air, and Soil Pollution*. **130**, 667-672.

Laenen, A., and Bencala, K.E. (2001) Transient Storage assessments of Dye Tracer Injections in Rivers of the Willamette Basin, Oregon: *American Water Resources Association*, **37(2),** 367-377.

Lund, L.J., Horne, A.J., and Williams, A.E. (2000) Estimating denitrification in a large constructed wetland using stable nitrogen isotope ratios: *Ecological Engineering*, **14**, 67-76.

Maitre, V., Cosandey, A.C., Desagher, E., and Parriaux, A., (2003) Effectiveness of groundwater nitrate removal in a river riparian area: the importance of hydrogeological conditions. *Journal of Hydrology*. **278**, 76-93.

McMahon, P.B. and Bohlke J.K. (1996) Denitrification and mixing in a stream aquifer system: effects on nitrate loading to surface water. *Journal of Hydrology*, **186**, 105-128.

Moffat, A.S. (1998) Ecology - Global nitrogen overload problem grows critical. *Science*. **279 (5353)**, 988-989.

Nascimento, C., Atekwana, E.A., and Krishnamurthy, R.V., (1997) Concentrations and isotope ratios of dissolved inorganic carbon in denitrifying environments. *Geophysical ResearchLetters*, **24(12)**, 1511-1514.

Norton, M.M., and Fisher, T.R., (2000), The effects of forest on stream water quality in two coastal plain watersheds of the Chesapeake Bay. *Ecological Engineering*. **14 (4)**, 337 362.

Ostrom, N.E., Hedin, L.O., Von Fischer, J.C., and Robertson, G.P. (2002) Nitrogen Transformations and NO_3^- Removal at a Soil-Stream Interface: A Stable IsotopeApproach. *Ecological Applications*, **12(4)**, 1027-1043.

Phillips, S.W. and Lindsey, B.D., (2003) The Influence of Ground Water on Nitrogen Delivery to the Chesapeake Bay. USGS Fact Sheet **FS-091-03**.

Pinay, G., Clement, J.C., and Naiman, R.J. (2002) Basic Principles and Ecological Consequences of Changing Water Regimes on Nitrogen Cycling in Fluvial Systems. *Environmental Management*. **30(4)**, 481-491.

Preston S.D. and Brakebill J.W. (1999) Application of Spatially Referenced Regression Modeling for the Evaluation of Total Nitrogen Loading in the Chesapeake Bay Watershed. *USGS Water-Resources Investigations Report* **99-4054**.

Reilly, T.E., Plummer, L.N., Phillips, P.J., and Brusenberg, E., (1994) The use of simulation and multiple environmental tracers to quantify groundwater flow in a shallow aquifer. *Water Resources Research*, **30**, 421-433.

Robinson D. (2001) $\delta^{15}N$ as an integrator of the nitrogen cycle. *Trends in Ecology and Evolution*. **16(3)**, 153-162.

Silva, S.R., Kendall, S., Wilkison, D.H., Ziegler, A.C., Chang, C.C.Y., and Avanzino, R.J., (2000) A new method for collection of nitrate from fresh water and the analysis of nitrogen and oxygen isotope ratios. *Journal of Hydrology,* **228**, 22-36.

Smith, R.A., Schwarz, G.E., and Alexander, R.B. (1997) Regional interpretation of water-quality monitoring data. *Water Res. Research.* **33(12),** 2781-2798.

Smith, S.V., Swaney, D.P., Talaue-McManus, L., Bartley, J.D., Sandhei, P.T., McLaughlin, C.J., Dupra, V.C., Crossland, C.J., Buddemeier, R.W., Maxwell, B.A., and Wulff, F. (2003) Humans, Hydrology, and the Distribution of Inorganic Nutrient Loading to the Ocean. *Bioscience.* **53(3),** 235-245.

Shedlock, R.J., (1993) The Delmarva Study: Assessing Regional Water Quality. *Geotimes*, **12/93**, 12-14.

Stumm, W., and Morgan J.J. (1996) Aquatic Chemistry: Chemical Equilibria and Rates in Natural Waters. Third Edition. John Wiley and Sons Inc., New York, NY.

Wang, Y., Huntington, T.G., Osher, L.J., Wassenaar, L.I., Trumbore, S.E., Amundson, R.G., Harden, J.W., McKnight, D.M., Schiff, S.L., Aiken, G.R., Lyons, B., Aravena, R.O., and Baron, J.S. (1998) Carbon Cycling in Terrestrial Environments, in Isotope Tracers in Catchment Hydrology Edited by Kendall and McDonnell, Elseiver Science.

Worman, A., Packman, A.I., Johansson, H., and Jonsson, K. (2002) Effect of flow induced exchange in hyporheic zones on longitudinal transport of solutes in streams an rivers: *Water Res. Research*, **38(1),** 1-15.

Yang, C., Telmer, K., and Veizer, J. (1996) Chemical dynamics of the "St. Lawrence" riverine system: δDH_2O, $\delta^{18}OH_2O$, $\delta^{13}C_{DIC}$, $\delta^{34}S_{sulfate}$, and dissolved $^{87}Sr/^{86}Sr$. *Geochmica et Cosmochimica Acta*, **60(5),** 851-866.

Zynjuk L.D. (1995) Chesapeake Bay: Measuring Pollution Reduction. *http://water.usgs.gov/wid/html/chesbay.html*